METABOLOMIC STUDIES OF SALIVA IN GINGIVITIS AND PERIODONTITIS

Alison M. McGuire

A thesis submitted to the faculty at the University of North Carolina at Chapel Hill in partial fulfillment of the requirements for the degree of Master of Science in the School of Dentistry (Periodontology).

Chapel Hill
2014

Approved by:

Steven Offenbacher

Silvana Barros

James Beck

ABSTRACT

Alison M. McGuire: Metabolomic Studies of Saliva in Gingivitis and Periodontitis
(Under the direction of Steven Offenbacher)

The aim of this study was to conduct metabolomic analysis of saliva during 3-week

induction and 4-week resolution of stent-induced, biofilm overgrowth (SIBO) in humans to

elucidate an association between changes in clinical disease and the salivary metabolome.

Five periodontal disease classifications were developed using probing depths and

bleeding on probing. SIBO was induced in 50 subjects for 21 days followed by oral hygiene

instruction for 28 days. Clinical indices and unstimulated saliva were collected weekly during

induction and biweekly during resolution. Samples were analyzed using metabolomic profiling

(liquid and gas chromatography mass spectrometry, Metabolon Inc).

SIBO was associated with marked, but reversible, increases in clinical indices. 281

metabolites were identified using metabolomic profiling. Eight metabolites demonstrated

significant changes including seven in the amino acid super-pathway (threonine, N-acetylserine,

serine, 5-oxoproline, histidine, glutamate and erythronate).

Analysis of the salivary metabolome may provide new mechanistic insights for

periodontal disease progression.

This thesis is dedicated to my husband, Leigh, my daughter, Charlotte and my parents.

ACKNOWLEDGEMENTS

I would like to thank my advisor, Distinguished Professor Dr. Steven Offenbacher, for his continuous support and source of inspiration. I would also like to thank my committee members, Associate Professor Dr. Silvana Barros and Distinguished Professor Dr. James Beck for their support.

TABLE OF CONTENTS

LIST OF TABLES

LIST OF FIGURES

LIST OF ABBREVIATIONS

ADP	Adenosine diphosphate
ATP	Adenosine triphosphate
BCAA	Branch-chain amino acids
BD-2	Beta-defensin 2
BGI	Biofilm-gingival interface
BGI-G	BGI-gingivitis
BGI-H	BGI-healthy
BGI-P1	BGI-periodontitis 1
BGI-P2	BGI-periodontitis 2
BGI-P3	BGI-periodontitis 3
BMI	Body mass index
BOP	Bleeding on probing
CAL	Clinical attachment level
CSF3	Colony stimulating factor 3
ENA-78	Epithelial-derived neutrophil-activating peptide-78
FDR	False discovery rates
GC/MS	Gas chromatography mass spectrometry
GCF	Gingival crevicular fluid
GI	Gingival index
IL	Interleukin
ITAC	Interferon inducible T-cell alpha chemoattractant
LC/MS	Liquid chromatography mass spectrometry

MCP-1	Monocyte chemoattractant protein-1
MIP-1β	Macrophage inflammatory protein-1β
MMP	Matrix metalloproteinase
MS	Mass spectrometry
NADH	Nicotinamide adenine dinucleotide
NADPH	Nicotinamide adenine dinucleotide phosphate
NHANES	National Health and Nutrition Examination Survey
PD	Probing depth
PI	Plaque index
RANTES	Regulated on activation, normal T cell expressed and secreted
RSD	Relative standard deviation
SIBO	Stent-induced, biofilm overgrowth
SOD2	Superoxide dismutase2
UNC	University of North Carolina
US	Unites States

CHAPTER 1: INTRODUCTION

Periodontal disease is a heterogeneous group of inflammatory conditions that affect tooth-supporting tissues and is broadly grouped into two major categories: gingivitis and periodontitis. Gingivitis is reversible and limited to superficial gingival tissues; periodontitis is non-reversible and features tissue destruction extending into the periodontal ligament and alveolar bone. Animal studies indicate that gingivitis is a precursor to periodontitis (Heijl, Rifkin, & Zander, 1976), however, human population studies have clearly shown that not all individuals with gingivitis linearly proceed to periodontitis (Löe, Anerud, Boysen, & Morrison, 1986; Socransky, Haffajee, Goodson, & Lindhe, 1984).

Estimations from NHANES III data suggest that approximately half (47.2%) of the US population has periodontal disease (Eke et al., 2012). Underestimations in previously reported periodontal disease prevalence may be due to inconsistent definitions of periodontal disease. For example, applying a threshold of 1mm CAL results in a prevalence of 99% while applying a threshold of greater than 7 mm CAL results in a prevalence of 7% (Albandar, Brunelle, & Kingman, 1999). Furthermore, use of partial mouth examinations such as the Ramfjord's Periodontal Disease Index (Ramfjord, 1967) may have led to underestimations in NHANES survey studies by 50% (Albandar, 2011).

There is a substantial body of literature published within the last 10 years that demonstrates associations between periodontal disease and a myriad of systemic diseases including diabetes, cardiovascular disease, stroke, kidney disease, and adverse pregnancy outcomes (Arce et al., 2010; Southerland et al., 2012). These associations have drawn the

attention of the medical field which has resulted in translational interdisciplinary research opportunities between medicine and dentistry (Williams & Offenbacher, 2000).

Periodontal disease is a multifactorial disease that is associated with several risk and susceptibility factors (Page & Kornman, 1997). Bacterial biofilm has historically been cited as the primary etiological factor for periodontal disease (Löe, Theilade, & Jensen, 1965), however, the amount of plaque does not necessarily correlate with periodontal disease severity (Offenbacher, 1996). Data from cohort studies indicate that a subset of individuals appear to exhibit a more pronounced host response to bacterial biofilm as compared to others who fail to respond (Offenbacher, Collins, & Arnold, 1993). Trombelli et al. (2004) first identified "high responders" and "low responders" in a randomized, split-mouth, localized experimental gingivitis model (Trombelli et al., 2004). These two groups were defined by upper and lower quartiles of GCF volume. During experimental gingivitis, "high responders" demonstrated a statistically significant increase in GI, angulated bleeding score, and GCF volume but not plaque index and cumulative plaque exposure when compared to "low responders". Evidence of this phenomenon was first published almost 50 years ago by Löe et al. (1965) in his classic experimental gingivitis study (Löe et al., 1965). Subjects refrained from daily tooth cleaning for three weeks to induce gingivitis. Using a clinical index (GI), three subjects developed gingivitis within 10 days ("high responders") whereas nine subjects developed gingivitis between 15-21 days ("low responders"). Differences in host susceptibility to gingivitis and periodontal disease may be traced to inter-individual differences in environmental exposures or genetic risk factors. In fact, genetic risk factors have been shown to account for approximately 50% of inter-individual variability in the expression of periodontal disease (Michalowicz et al., 2000). Observational studies suggest that a risk for advanced periodontitis may be elevated in patients

with certain genetic biomarkers or polymorphisms (interleukin-1β) however the risk conferred by these markers are not consistent among different populations (Kinane & Hart, 2003). In fact, Papapanou et al. (2004) conducted a pilot study evaluating gene expression signatures in gingival tissues obtained from two subsets of periodontal disease patients: chronic and aggressive. This group concluded that gene expression techniques may be useful in the identification of different subclasses of periodontal diseases and better allow clinicians to distinguish health from disease (Papapanou et al., 2004). Collectively, these studies provide evidence for the potential utility of biochemical mediators for periodontal diagnosis.

The intent of this study is to elucidate the association between clinical disease status and the salivary metabolome by conducting metabolomic analysis on saliva from 50 subjects with periodontal health, gingivitis and three stages of periodontal disease. We hypothesize that metabolomic signatures exist for five disease categories (health, gingivitis, mild, moderate and severe periodontitis) which may be applied to novel salivary diagnostic tests. As a secondary goal, we were interested in identifying new candidate biomarkers within saliva, which co-vary with the changes in clinical status.

CHAPTER 2: LITERATURE REVIEW

Section 2.1: Oral fluids

Oral fluids are composed predominantly of salivary gland secretions but also variable amounts of bronchial and nasal secretions, gingival epithelial cells, food debris, and GCF products including serum transudate, microbial, and host products (Kaufman & Lamster, 2002; Offenbacher et al., 2010). Inflammatory mediators in GCF have been evaluated as potential diagnostic markers for periodontal disease activity and progression. Offenbacher et al. (2007) defined BGI categories based on PD and BOP that were validated by multivariate models using clinical, microbial, inflammatory, and host-response data (Offenbacher et al., 2007). This classification was developed to investigate the underlying biology since it uses PD and BOP rather than CAL, which also represents past disease. Offenbacher et al. (2010) conducted an experimental gingivitis study using the SIBO model with subjects diagnosed with gingivitis and applied immunoadsorbant bead suspension array multiplexing tools to simultaneously analyze 33 inflammatory mediators within each GCF sample to evaluate changes in GCF composition over time (Offenbacher et al., 2010). Gingivitis induction was associated with a significant 2.6-fold increase in IL-1β, 3.1-fold increase in IL-1α and significant decreases in select MMP's and chemokines (including IL-8, MIP-1β, ENA-78, MCP-1, and RANTES) that returned to baseline values following resolution of experimental gingivitis. Increases in IL-1β and IL-1α during gingivitis induction have been described previously (Heasman, Collins, & Offenbacher, 1993; Offenbacher et al., 2007). Decreased chemokines may represent increased degradation in the sulcus or a shift in chemokine compartmentalization between tissues and GCF. Decreases in the

abovementioned chemokines, which are chemotactic for leukocytes, suggests that experimental gingivitis induces a transient, but reversible suppression of chemotaxis. This study identified IL-1β, IL-1α, and select MMP's and chemokines as potential candidate biomarkers for gingivitis induction within the GCF.

Section 2.2: Advancements in molecular biology technologies

Due to advancements in molecular biology and, in particular, high-throughput technologies, systems biology has emerged in the last decade to evaluate biological systems at the level of the genome, transcriptome, proteome, glycome, metabolome, and lipidome which have been termed genomics, transcriptomics, proteomics, glycomics, metabolomics, and lipidomics respectively (Wu, Zhao, Wang, Zhou, & Chen, 2011). Gingival transcriptome patterns during induction and resolution of experimental gingivitis were described by Offenbacher et al. (2009) using the SIBO model (Offenbacher et al., 2009). Briefly, gingival biopsy samples were collected from 14 subjects at different sites within each subject at baseline (Day 0), peak of gingivitis (Day 28), and resolution (Day 35) and processed using whole-transcriptome gene-expression arrays. During induction, there was a significant transient increase in expression levels of transcripts that code for inflammatory cytokines including in IL-1β, IL-1α, IL-8, RANTES, CSF3, and SOD2 and a decreased expression of IL-10, ITAC, MMP-10, and BD-2.

Section 2.3: Metabolomics

Overview

Metabolomics is the study of small molecules in biological systems including amino acids, peptides, carbohydrates, fatty acids, metabolites, xenobiotics, and exogenous chemical

agents (Lawton et al., 2008; Ryals, Lawton, Stevens, & Milburn, 2007). The goal of metabolomics is to characterize the metabolic state of a subject via extraction, identification, and quantification of all small molecule compounds from a biological sample (Ryals et al., 2007). There are advantages of metabolomics over other technologies such as functional genomics, transcriptomics, and proteomics. For example, metabolomics provides a biochemical signature that includes the effects of genetics, lifestyle, diet, and environmental factors in an individual (Ryals et al., 2007). To date, blood, urine, gingival crevicular fluid, saliva, amniotic fluid, cerebrospinal fluid, tissues, cell cultures, and plants have been analyzed by metabolomic profiling (Ryals et al., 2007). This is a rapidly evolving technology that has been used increasingly in drug development and diagnosis of systemic disease (Lawton et al., 2008; Morris & Watkins, 2005). For example, this technology has been applied to cardiovascular disease and diabetes research (Dunn, Goodacre, Neyses, & Mamas, 2011). It has also been used to investigate diagnostic markers for psychological diseases such as depression (Paige, 2007). Analysis of biological metabolites for disease diagnosis and monitoring of disease status is not novel. For example, blood glucose and cholesterol levels have been used for decades in the diagnosis and disease monitoring for diabetes and heart disease respectively. However, advancements in technology have allowed for analysis of a much wider variety of metabolites in a given sample (Lawton et al., 2008).

Metabolomic profiling: Technology

Metabolomic profiling includes integration of targeted metabolomic analysis and non-targeted metabolomic analysis. Targeted metabolomic analysis provides absolute concentrations of a small number of known metabolites (Lawton et al., 2008); non-targeted metabolomic

6

profiling provides a relative concentration of a large number of small molecules, known and unknown, in a biological sample that permits a broader examination of metabolism (Sha et al., 2010). Both non-targeted and targeted analyses apply LC/MS and GC/MS. Briefly, metabolites extracted from a sample are identified by matching the ion's chromatographic retention index and mass spectral fragmentation signatures with a reference library. For molecules not found in the reference library, new library entries are added (Barnes et al., 2009). Quality control is essential for several reasons. First, metabolites in biological systems are found in widely varying concentrations with different molecular size, functional moieties, lipophilicity, volatility, or other physicochemical parameters from which they must be extracted while maintaining their structural integrity and relative abundances (Fiehn et al., 2008). Secondly, some compounds, such as ATP, ADP, NADH and NADPH are susceptible to oxygen degradation during sample preparation. Other compounds, such as sugar phosphates, cysteine and ascorbate are prone to degradation by residual enzymatic activity, heat and oxidation (Fiehn et al., 2008). To overcome these challenges, quality control samples, including internal standards and endogenous biochemicals, are analyzed alone and in conjunction with the samples to measure variation between experiments (Lawton et al., 2008). Some variation is acceptable and is due to deviation in sample processing, instrument or data processing (Dunn, Wilson, Nicholls, & Broadhurst, 2012). Extended details of methods are included in Appendix 3.1.1.

Metabolomic profiling: Developing metabolomic signatures in GCF

Inflammatory biomarkers within oral fluids have been evaluated as a potential diagnostic aid for periodontal disease (Barnes et al., 2009). These biomarkers cover a range of biological processes that would provide insight as to the presence, absence, and severity of disease and

would allow for the development of diagnostic tests. Barnes et al. (2009) applied metabolomic

profiling to GCF samples collected from healthy, gingivitis, and periodontitis sites in humans via

LC/MS and GC/MS and identified metabolomic signatures associated with host-bacterial

interactions (Barnes et al., 2009). Of the 228 metabolites detected, 53 metabolites (23%)

demonstrated significant differences between subjects with gingival health, gingivitis, and

periodontitis defined as sites with PD≤3mm, absent BOP; PD≤3mm, BOP present; and

PD≥5mm, BOP present, respectively after correcting for multiple comparisons (FDR, $q < 0.05$).

Most metabolites with altered concentrations at gingivitis sites demonstrated intermediate levels

between health and periodontitis, which suggests that metabolomic changes are on a continuum.

Inosine, hypoxanthine, xanthine, guanosine, and guanine were upregulated at the disease sites

which indicated accelerated metabolic flux of the purine degradation pathway. In accordance

with these changes, oxygen levels were depleted and reactive oxygen species were elevated by

xanthine oxidase. Levels of anti-oxidants including reduced and oxidized glutathione, ascorbic

acid, and uric acid were reduced. These findings suggested an acceleration of reactive oxygen

species that have been shown to be involved in the pathogenesis of other diseases such as

cardiovascular disease, ischemic-reperfusion injury, diabetes, hypertension and inflammatory

disease (Ren, Zhang, Cui, & Mu, 2013). Levels of putrescine and cadaverine, which are the end-

products of amino acid degradation, were also upregulated by disease. The authors suggested

that host tissues upregulate the purine degradation pathway as a defense mechanism against

oxidant-sensitive bacterial pathogens (Barnes et al., 2009; Stevens et al., 2000). In a follow-up

study, Barnes et al. (2010) evaluated the effect of triclosan-containing dentifrice on the

metabolomic profile of subjects with gingivitis and demonstrated decreased levels of inosine,

lycine, putrescine, and xanthine as early as one week after implementing the triclosan-containing dentifrice (Barnes, 2010).

Metabolomic profiling: Developing metabolomic signatures in saliva

These mediators are detectable in saliva, albeit at a much lower concentration, which opens the possibility for a salivary diagnostic to monitor periodontal status. Barnes et al. (2011) conducted a study evaluating salivary metabolites in human subjects with periodontal health and periodontitis. A total of 68 unstimulated saliva samples were collected from 34 periodontally healthy and 34 periodontitis subjects. Of the 390 metabolites that were detected, seven metabolites demonstrated significant differences between subjects with periodontal health and periodontitis (FDR, q<0.05). Five of the seven metabolites were derived from four different superfamilies (leucylisoleucine from the dipeptide superfamily, mannose and glucose from the carbohydrate superfamily, arachidonate from the lipid superfamily, and allantoin from the nucleotide superfamily) while two were previously unnamed. Metabolites from several pathways demonstrated trending changes (t-test, $p<0.05$) including elevated mono- and oligosaccharides, dipeptides, products of glycerophopholipid and triacylglycerol degradation including fatty acids arachidonate and docosapentaenoate, and nucleotides. This publication was the first to report on metabolomic profiling of saliva and suggested that a number of different metabolites could be investigated as candidate biomarkers for a salivary diagnostic tool. Integrating metabolomic profiles of the GCF and saliva may provide a comprehensive biochemical basis for understanding the pathogenesis of periodontal disease and limit the number of candidate biomarkers for a diagnostic aid (Barnes et al., 2011).

CHAPTER 3: MANUSCRIPT

Section 3.1: Introduction

Human saliva contains salivary gland secretions but also variable amounts of bronchial and

nasal secretions, gingival epithelial cells, food debris, and GCF products; including serum

transudate, microbial, and host products (Kaufman & Lamster, 2002; Offenbacher et al., 2010).

In the last decade, the application of systems biology has been used to evaluate biological

systems at the level of the genome, transcriptome, proteome, glycome, metabolome, and

lipidome (Wu, Zhao, Wang, Zhou, & Chen, 2011). Recently, the application of whole-

transcriptome gene-expression arrays has been used to characterize gingival transcriptome

patterns in gingival tissue (using gingival biopsies) during induction and resolution of

experimental gingivitis using the SIBO model (Offenbacher et al., 2009). During induction, a

significant transient increase in expression levels of transcripts that code for inflammatory

cytokines including in IL-1β, IL-1α, IL-8, RANTES, CSF3, and SOD2 and a decreased

expression of IL-10, ITAC, MMP-10, and BD-2 was noted. For ease of collection, these

technologies have been applied to GCF and saliva.

Metabolomics is the study of small molecules in biological systems including amino

acids, peptides, carbohydrates, fatty acids, metabolites, xenobiotics, exogenous chemical agents

(Lawton et al., 2008; Ryals, Lawton, Stevens, & Milburn, 2007). Barnes et al. (2009) applied

metabolomic profiling to GCF samples collected from healthy, gingivitis, and periodontitis sites

in humans via LC/MS and GC/MS and identified metabolomic signatures associated with host-

bacterial interactions (Barnes et al., 2009). Of the 228 metabolites detected, 23% demonstrated

significant differences between subjects with gingival health, gingivitis, and periodontitis. This study showed accelerated metabolic flux of the purine degradation pathway, depletion of oxygen levels, elevated reactive oxygen species and reduced levels of anti-oxidants (Barnes et al., 2009). Additionally, metabolites from the amino acid super-family were increased while metabolites from the glutathione pathway were reduced (Barnes et al., 2009). In the first publication to report on metabolomic profiling of saliva, Barnes et al. (2011) applied metabolomics to saliva samples collected from human subjects with periodontal health and periodontitis. Among the 390 metabolites detected, 0.02% demonstrated significant differences between subjects with periodontal health and periodontitis. The data indicated changes in biochemicals from several different pathways including dipeptides, carbohydrates, lipids and nucleotides which suggested that a number of different metabolites could be investigated as candidate biomarkers for a salivary diagnostic tool (Barnes et al., 2011). The experimental gingivitis model has been applied many times since it was first introduced in the landmark study by Löe *et al.* (Löe et al., 1965). This model has been adapted to include the use of intra-oral stents to be worn only during routine oral hygiene measures that cover selected teeth (Burrell & Walters, 2008) to limit the extent of gingival inflammation to selected posterior regions of the mouth. In this study, we applied the SIBO model in conjunction with metabolomic profiling from human saliva samples to elucidate the association between clinical disease status and the salivary metabolome. This was a hypothesis-generating experiment with the goal of identifying metabolomic signatures in five disease categories (health, gingivitis, mild, moderate and severe periodontitis). As a secondary goal, we were interested in identifying new candidate biomarkers within saliva, which co-vary with the changes in clinical status.

Section 3.2: Materials and Methods

Clinical study design and patient enrollment

      This study design represents a modification of the original experimental gingivitis study as described by Löe *et al.*(Löe et al., 1965). We recruited and enrolled subjects who were systemically healthy with periodontal diagnoses of health, gingivitis, mild, moderate or severe periodontitis in this study conducted at the UNC Center for Oral and Systemic Diseases. The study design included a 2-week hygiene phase, a 3-week induction phase using two stents and a 4-week resolution phase to reinstitute oral hygiene and reverse gingival inflammation. The protocol and informed consent were approved by the Institutional Review Board at UNC Chapel Hill. 175 subjects (115 females and 60 males; aged 19-68 years) were enrolled in the study and 163 subjects completed the experimental protocol between July 2009 and October 2010. The subjects included in this study are a subset of a larger study; the data collected from all 163 subjects were analyzed elsewhere. Samples were analyzed for a total of 50 subjects (33 females and 17 males; 19-53 years); subjects were randomized by each BGI strata to a total of 10 subjects per stratum. Eligibility criteria included: adult male or females; age range: 18 to 75 years; good general health; ≥8 teeth in a functional dentition with a minimum of 3 adjacent teeth with interproximal papilla in each posterior sextant; that may be classified into one of the following five categories: BGI-H (all PD≤3mm, BOP<10%), BGI-G (all PD≤3mm, BOP≥10%), BGI-P1 (≥1 site with PD>3mm, BOP≤10%), BGI-P2 (≥1 site with PD>3mm, 50%≥BOP>10%), BGI-P3 (1≥ site with PD>3mm, BOP>50%). Exclusion criteria included: (1) individuals who have a chronic disease with oral manifestations or active infectious diseases such as hepatitis, HIV or tuberculosis; (2) individuals who exhibit gross oral pathology; (3) treatment with antibiotics for any medical or dental condition within one month prior to the study; (4) chronic

treatment (i.e., two weeks or more) with any medication known to affect periodontal status (e.g., phenytoin, calcium antagonists, cyclosporin, anticoagulants, non-steroidal anti-inflammatory drugs, high dose aspirin such as >100mg per day) within one month prior to the study; (5) ongoing medications initiated less than three months prior to enrollment (i.e., medications for chronic medical conditions must be initiated at least three months prior to enrollment); (6) participants with clinically significant organ disease including impaired renal function, and/or any bleeding disorder; (7) severe unrestored caries, or any condition that is likely to require antibiotic treatment during the study, including the need for prophylactic antibiotic; (8) individuals who use any tobacco products or who have used tobacco products within the previous six months of the study; (9) individuals who are pregnant, or expect to become pregnant, within the next three months and individuals nursing. Participants were excluded from the study or analysis if any of the following conditions occurred: (1) changes in the participant's medical status or medications; (2) use of any antibacterial rinses; (3) use of non-study dentifrices, toothbrushes or dental floss during the no-hygiene and resolution phases of the study; (4) use of irrigating devices or other interdental aids; (5) participant's inability or noncompliance to wear their stents or shields over the selected no-hygiene sextants during daily brushing procedures; (6) use of oral antibiotics and non-steroidal anti-inflammatory drugs during the trial. Acute use of oral acetaminophen was permitted. Participants requiring treatment for an acute medical or dental condition during the study were withdrawn from the trial.

Patient protocol and procedures

At the screening visit (visit 1) informed consent was obtained, medical history, height, weight and vital signs were collected, a full-mouth clinical examination was performed and

impressions were made for stent fabrication. Full mouth-examination included oral cancer screening, GI (Löe & Silness, 1963), PI (Silness & Löe, 1964), PD, CAL and BOP scores (yes/no) at each of six sites per tooth. Customized stents were fabricated for each subject to encourage participant compliance during daily brushing procedures. Stents resembled an acrylic occlusal guard but extended to cover approximately 2 mm over gingival margins. Stents formed a seal and rested on the gingiva, but were relieved on the tooth and tissue side except for occlusal surfaces to avoid disturbing plaque or gingival tissues. Within two weeks at visit 2 (Day -14) the exam was repeated and biological samples were collected: 3 mL of whole, unstimulated saliva was collected. At visit 2, standardized study products including fluoride dentifrice and a toothbrush were dispensed and subjects were instructed on toothbrush technique. Following a 2-week hygiene phase, participants returned for the baseline (Day 0) visit. At this visit subjects were given two stents and instructions for use. From this point forward for a 3-week, no-hygiene phase, subjects abstained from all oral hygiene procedures in two posterior sextants via placement of acrylic stents. At baseline (Day 0), saliva was collected, clinical exams performed, vitals, adverse events recorded and medical histories updated. All participants refrained from all oral hygiene procedures (i.e., tooth brushing, flossing or use of interdental aids) in two sextants that were preselected as the upper right (teeth #1-6) and lower right (teeth #27-32); if there were fewer than four teeth in a sextant then the contralateral sextant was selected. Participants were directed to continue plaque removal procedures to the remaining four sextants using the fluoride dentifrice provided at visit 2 (Day -14). Participants were instructed to discontinue flossing altogether to prevent inadvertently flossing stent teeth. Subjects were seen on Day 7, 14 and 21 for saliva collection during the induction phase and clinical exams were performed at each visit to assure patient safety and compliance. At Day 21, subjects were provided oral hygiene

14

instruction, both verbally and in writing, and advised to brush their entire dentition twice a day and continue to abstain from flossing during the 4-week resolution phase (Days 21-49). Subjects returned on Day 35 for repeated clinical exam and biological sampling of saliva. Subjects returned on Day 49 (four weeks after reinstating oral hygiene) for repeated clinical exam and biological sampling of saliva. Upon exit of the study, oral prophylaxis or scaling root planing was performed on all subjects to regain periodontal health. Day 21 represents the peak of gingival inflammation induction while Day 49 represents the peak of gingival inflammation resolution.

Saliva samples were collected from subjects on Day -14, 0, 7, 14, 21, 35 and 49. At each of these time points, approximately 3 mL of unstimulated saliva was collected into a 15 mL conical tube. Subjects refrained from eating, drinking, chewing gum, breath mints, etc., or performing oral hygiene procedures for at least one hour prior to saliva collection. This request was made after consenting for the first sample collection. Saliva was collected using a 15 mL polypropylene tube. The subject spit into the collection vessel but was instructed to avoid coughing up mucus. During saliva collection, the collection vessel was kept at room temperature, centrifuged and aliquoted into three samples of 0.5 mL in each tube. Remaining saliva was aliquoted into a fourth tube and samples were stored at -80C.

Examiner training and calibration

Clinical examiners were calibrated before commencement of the study for training of study procedures and for documentation of acceptable intra- and inter-examiner measurement reliability. This examiner calibration and training is under a separate IRB-approved protocol that is performed within the General and Oral Health Center at UNC School of Dentistry. Examiners

were standardized on measurements of the PI, GI, PD, CAL and BOP. The three participating examiners were found to have an intra-class k coefficient of agreement between 0.94-0.98 for PD and between 0.77-0.97 for CAL measurements, as compared with the gold standard examiner. Clinical parameters were measured using a manual UNC-15 periodontal probe. For experimental SIBO measures, these parameters were measured at six sites per tooth for teeth within the two experimental SIBO sextants and for teeth in the other four sextants for control purposes. Examiners were masked to the subject's BGI category.

Analysis of the salivary metabolome

Metabolomic analyses were conducted at Metabolon, Inc. (Durham, NC). Samples were subjected to both non-targeted and targeted analysis via LC/MS and GC/MS as described by Evans et al. (2012) (Evans, Mitchell, Dai, & DeHaven, 2012). Saliva samples were analyzed in duplicate from timepoints -14, 0, 7, 14, 21, 35 and 49 days for each subject. Results were reported as raw concentrations of metabolites for five groups (BGI-H, BGI-G, BGI-P1, BGI-P2, and BGI-P3) at seven time points (Day -14, 0, 7, 14, 21, 35 and 49) which provided data at baseline, induction and resolution. All laboratory analyses were performed masked from sample, visit or subject information. Extended details of methods are included in Appendix 3.1.1.

Statistical analysis

Statistical analyses was performed using SPSS 22.0 software (SPSS, Inc., Chicago, IL). For demographic variables, a chi-squared test (χ^2) was used to determine statistical significance between categorical variables and general linear models were used to determine statistical significance between means. For clinical indices, general linear models were used to compare

16

days 7–21 with baseline and days 35 and 49 with peak of induction (day 21). Statistical significance is reported for $p<0.05$, $p<0.001$, and $p<0.0001$. Paired t-tests were used to compare mean metabolites at peak of induction with baseline and peak of resolution with peak of induction. FDR was applied to correct for multiple comparisons and was reported as q-values. Since very few changes were statistically significant by FDR, unadjusted p-values were reported to demonstrate trending changes. Covariance matrices were applied to describe correlations between changes in metabolites and changes in clinical indices at peak of induction (Day 21). r values were reported with corresponding p-values and q-values determined by paired t-tests and FDR respectively.

Section 3.3: Results

Study implementation

357 subjects were screened to reach the target enrollment. Subjects were recruited in two phases to provide interim data on disease states: (1) BGI-P1, BGI-P2, BGI-P3; (2) BGI-H, BGI-G. Participants were recruited by advertisement including email, flyers, internet postings and newspaper ads from the patient, student, and staff population at UNC Chapel Hill and the general population. 182 subjects did not meet the inclusion criteria and were excluded from the study. 175 subjects met the inclusion criteria, were enrolled in the study, and were classified by BGI category: BGI-H (36 subjects), BGI-G (34 subjects), BGI-P1 (33 subjects), BGI-P2 (37 subjects) and BGI-P3 (35 subjects). In the BGI-H category, two subjects dropped out due to medical conditions; in the BGI-G category, one subject dropped out due to time constraints; in the BGI-P1 category, one subject dropped out since she was not comfortable abstaining from oral hygiene; in the BGI-2 category, five subjects dropped out due to time constraints; in the BGI-P3

17

category, three subjects dropped out due to time constraints. 163 subjects completed the study in the following BGI categories: BGI-H (34 subjects), BGI-G (33 subjects), BGI-P1 (32 subjects), BGI-P2 (32 subjects) and BGI-P3 (32 subjects). Patient flow is illustrated in Figure 1. Samples were analyzed for a total of 50 subjects; subjects were randomized by each BGI strata to a total of 10 subjects per stratum. The mean age of the 50 subjects was 31.0 (standard deviation, 9.2), comprising 26 African Americans, 20 Caucasians, four other, 33 females and 17 males. Demographic information is provided in Table 1.1. Among the demographic variables presented in Table 1.1, age, former smoking and BMI are potential biases. Baseline clinical indices by BGI category are provided in Table 1.2,

Changes in clinical signs during induction and resolution of experimental SIBO

The SIBO model has practical advantages as compared with the traditional experimental gingivitis model described by Löe et al. (1965) in which total abstinence from oral hygiene procedures was required. Specifically, subjects prefer to be able to limit the extent of gingival inflammation to selected posterior regions of the mouth and to be able to use dentifrice and normal brushing on the remainder of the dentition and tongue to improve oral freshness (Löe et al., 1965). During the 3-week induction phase, SIBO was associated with an overall increase in clinical signs of inflammation and plaque scores that was limited to the stent area (Table 2.1). Clinical indices during induction and resolution of experimental SIBO by BGI category are shown in Table 2.2. Using general linear models, the increases seen in PI and GI are statistically significant by one week and increased in magnitude through Day 21 ($p<0.001$) in each of the BGI categories with the exception of BGI-P3. After reinstating oral hygiene at Day 21, there is a statistically significant decrease in mean PI and GI in each of the BGI categories at Days 35 and

18

49 as compared with Day 21 and a return to baseline values ($p < 0.05$). A similar trend was seen

for BOP which achieved statistical significance at Day 21 in each of the BGI categories with the

exception of BGI-P3 ($p < 0.05$). PI, GI, BOP, PD and CAL trends are depicted in Figures 2.1-

2.5. Slight changes in PD and CAL did not reach statistical significance. Thus, there was

induction of experimental SIBO under the stent that was fully and readily reversed by reinstating

oral hygiene. None of the subjects required scaling root planing at Day 49.

Changes in metabolome during induction and resolution of experimental SIBO

281 metabolites, that represent breakdown products of various super-pathways

(carbohydrate, lipid, amino acid, xenobiotics, nucleotide, cofactors and vitamins) and sub-

pathways, were quantified at each time point. At baseline, there were no significant differences

in metabolite levels between BGI categories (FDR, $q < 0.05$). When mean metabolite levels were

analyzed, without stratifying by BGI category, eight metabolites demonstrated significant

changes between baseline and peak of induction (Day 21) using FDR-adjusted p-values (q-

values) (Table 3.1). Seven of these eight metabolites are in the amino acid super-pathway. No

metabolites demonstrated significant changes between peak of induction (Day 21) and peak of

resolution (Day 49) when applying FDR (data not reported).

When mean metabolite levels were stratified by BGI category, no metabolites

demonstrated significant changes between baseline and peak of induction (Day 21) or peak of

induction (Day 21) and peak of resolution (Day 49) when applying FDR. Appendix 3.2 includes

metabolite levels stratified by BGI category that demonstrated trending changes (unadjusted p-

values < 0.05). Table 3.2 demonstrates top five trending changes in metabolite levels between

baseline and peak of induction while Table 3.3 demonstrates trending changes in metabolite

19

levels between peak of induction and peak of resolution. A summary of changes of metabolites from biochemical pathways altered by experimental SIBO is depicted in Table 3.4.

When generalized linear models and FDR were applied adjusting for age, BMI and former smoking, no changes in metabolites remained statistically significant ($q < 0.05$). It is possible that sample size was insufficient to capture significant changes when such rigorous statistical analyses were applied.

Mean levels of threonine, N-acetylserine, and serine from the glycine, serine and threonine metabolism sub-pathway decreased from baseline to peak of induction (Day 21) ($q < 0.05$). The glycine, serine and threonine metabolism sub-pathway is illustrated in Figure 4b. From this pathway, glycine demonstrated a trending decrease from baseline to peak of induction and increase from peak of induction to peak of resolution in the BGI-H category (unadjusted $p < 0.05$) (Appendix 3.2). Additionally, homoserine, N-acetylglycine and O-acetylhomoserine, demonstrated trending changes in various BGI categories. There was a very strong correlation at peak of induction between mean levels of threonine and serine (r = 0.874) but weak correlations at peak of induction between mean levels of threonine and N-acetylserine (r = 0.247) and between N-acetylserine and serine (r = 0.071).

Mean levels of histidine, from the histidine metabolism sub-pathway, were decreased from baseline to peak of induction ($q = 0.03$). The histidine metabolism sub-pathway is illustrated in Figure 4c. Histidine metabolites include trans-urocanate and cis-urocanate. Trans-urocanate demonstrated a trending decrease from peak of induction (Day 21) to peak of resolution (Day 49) without stratifying by BGI category (unadjusted $p < 0.05$) while cis-urocanate demonstrated a trending decrease from peak of induction (Day 21) to peak of resolution (Day 49) in the BGI-P1 category (unadjusted $p < 0.05$). Mean levels of 5-oxoproline,

from the glutathione metabolism sub-pathway, decreased from baseline to peak of induction ($q =$ 0.02). The glutathione metabolism pathway is illustrated in Figure 4d. Mean levels of glutamate were decreased from baseline to peak of induction ($q = 0.03$) (Figure 4a). Glutamate is included in several pathways including the histidine metabolism sub-pathway, the glutathione metabolism sub-pathway, the purine metabolism sub-pathway, and the alanine, aspartate and glutamine metabolism sub-pathway. Glutamate demonstrated a trending decrease from peak of induction (Day 21) to peak of resolution (Day 49) in the BGI-G category (unadjusted $p < 0.05$). Additionally, glutamine, a metabolite that shares several pathways with glutamate, demonstrated a trending decrease from baseline to peak of induction without stratifying by BGI category (unadjusted $p < 0.05$). There was a moderate correlation at peak of induction between mean levels of metabolites glutamate and 5-oxoproline (r = 0.874) which are included in the glutathione metabolism sub-pathway (Figure 4d).

Mean levels of erythronate, from the aminosugars metabolism sub-pathway, were decreased from baseline to peak of induction ($q = 0.03$). Trending decreases were seen in the BGI-P1 category from peak of induction to peak of resolution (unadjusted $p < 0.05$).

Mean levels of tyrosine, from the phenylalanine and tyrosine metabolism sub-pathway, were decreased from baseline to peak of induction ($q < 0.05$). From the phenylalanine metabolism sub-pathway, several metabolites including phenyllactate, P-cresol sulfate, and phenylacetate demonstrated trending decreases from baseline to peak of induction in the BGI-H category.

Trending increases and decreases in metabolite levels from baseline to peak of induction (Day 21) and from peak of induction (Day 21) to peak of resolution (Day 49) were indicated as blue and red p-values, respectively. Interesting findings include BCAAs isoleucine and valine

which showed trending, although not statistically significant, decreases at peak of induction (Day 21) as compared to baseline in the BGI-H category (unadjusted $p < 0.05$). Similarly, 3-hydrohyisobutyrate and citramalate, which are members of the valine, leucine and isoleucine metabolism pathway, also showed trending, although not statistically significant, decreases at peak of induction (Day 21) as compared to baseline in the BGI-H category (unadjusted $p < 0.05$).

Changes in clinical indices that co-vary with changes in metabolites

Covariance matrices were applied to describe correlations between mean changes in metabolites and changes in clinical indices at peak of induction (Day 21). When changes in mean metabolites were analyzed without stratifying by BGI category, no metabolites with $q < 0.05$ were noted (Table 4.1). A weak negative correlation was noted between changes in CAL at peak of induction and mean changes in glycine (r = -0.34, $p = 0.02$) and taurine (r = -0.3, $p = 0.03$) which were statistically significant. A weak positive correlation was noted between changes in BOP at peak of induction and mean changes in 5-oxoproline (r = 0.25, $p = 0.08$) and cis-uroconate (r = 0.27, $p = 0.06$) which was not statistically significant (data not reported).

When changes in metabolite levels were stratified by BGI category, two metabolites demonstrated very strong positive correlations that were statistically significant with changes in BOP in the BGI-P1 group: 3-aminoisobutyrate (nucleotide super-family, r = 0.92, $p < 0.01$, $q = 0.03$) and 1,3-diaminopropane (amino acid super-family, r = 0.91, $p < 0.01$, $q = 0.03$) at peak of induction (Appendix 3.3). 3-aminoisobutyrate demonstrated a trending decrease in BGI-P1 from baseline to peak of induction while 1,3-diaminopropane demonstrated a trending decrease in BGI-H from baseline to peak of induction (t-test, p< 0.05).

In the BGI-H group, a strong positive correlation was noted between changes in BOP and mean changes of glutamate (r = 0.69, p = 0.03) and glutamine (r = 0.64, p = 0.04). Additionally, a strong positive correlation was noted between changes in BOP and threonine in BGI-P2 (r = 0.68, p = 0.03), between changes in PI and GI and histidine in BGI-H (r = 0.71, p = 0.02 and r = 0.69, p = 0.03 respectively), and between changes in PI and 5-oxoproline in BGI-P1 (r = 0.69, p = 0.03).

Section 3.4: Discussion

Proteolytic bacteria degrade nitrogenous compounds producing peptides and amino acids that can be further metabolized by the bacterium and serve as additional nutrient sources. When mean metabolite levels were analyzed by FDR, without stratifying by BGI category, eight metabolites (0.03%) demonstrated significant decreases between baseline and peak of induction, including seven metabolites from the amino acid super-pathway. At baseline, there were no significant differences in metabolite levels between BGI categories. As such, it is not possible to differentiate between disease states with cross-sectional measurements of metabolites at baseline. This finding is in agreement with Barnes et al. 2011 who demonstrated very few significant differences between disease categories (0.02% of metabolites differed significantly between periodontal health and periodontitis). When mean metabolites were stratified by BGI category and analyzed by FDR, no changes between baseline, peak of induction and peak of resolution were statistically significant but trending changes were noted (Tables 3.2, 3.3). It appears that the power of this study was insufficient to demonstrate statistically significant changes by BGI category by FDR. Trending changes may implicate important metabolic pathways and should not be ignored.

Threonine, N-acetylserine, and serine, from the serine and threonine metabolism sub-pathway, decreased from baseline to peak of induction ($q < 0.05$). Threonine bridges the glycine, serine and threonine metabolism sub-pathway and the valine, leucine and isoleucine biosynthesis sub-pathway. Interestingly, trending decreases of isoleucine, valine, 3-hydroxyisobutyrate and citramalate, from the valine, leucine and isoleucine metabolism sub-pathway, were noted in the BGI-H category from baseline to peak of induction. Additionally, glycine, which is an intermediate metabolite between serine and threonine, demonstrated a trending decrease from baseline to peak of induction and increase from peak of induction to peak of resolution in the BGI-H category (unadjusted $p < 0.05$). The statistically significant decrease in threonine, N-acetylserine, and serine and trending non-significant decrease in glycine, isoleucine, valine, 3-hydrohyisobutyrate and citramalate may represent a feature of the gingival bacterial populations reliance on protein breakdown and amino acid catabolism for energy and specifically the serine and threonine metabolism and valine, leucine and isoleucine metabolism sub-pathways. The very strong correlation at peak of induction between mean levels of threonine and serine ($r = 0.874$) strengthens this postulation. These findings are in contrast with those of Barnes et al. (2011) who studied salivary metabolites in human subjects with periodontal health and periodontitis and demonstrated that while dipeptides were elevated, amino acids were unchanged with the exception of cysteine, which was elevated (Barnes et al., 2011).

Barnes et al. (2009) conducted metabolomic analysis of GCF samples collected from healthy, gingivitis, and periodontitis sites in humans (Barnes et al., 2009). Levels of putrescine and cadaverine, which are the end-products of amino acid degradation, were upregulated by disease. The authors suggested that host tissues upregulate the purine degradation pathway as a defense mechanism against oxidant-sensitive bacterial pathogens. Interestingly, neither

putrescine nor cadaverine demonstrated statistically significant changes at peak of induction and peak of resolution in this study (data not reported). Cadaverine demonstrated a trending increase at peak of induction compared to baseline and a trending decrease at peak of resolution as compared to peak of induction when samples were not stratified by BGI category (unadjusted p <0.05). It is possible that reduced concentrations of these metabolites in saliva as compared with GCF accounts for this effect.

Mean changes of glutamate were statistically significantly decreased from baseline to peak of induction. Since glutamate is an amino acid that is commonly metabolized by oral bacteria (Takahashi, Sato, & Yamada, 2000), the decrease observed in this study strengthens the postulation that gingival bacterial populations rely on amino acid catabolism for energy and specifically glutamate for carbon and sulfur metabolism. When samples were pooled, glutamine demonstrated a trending decrease from baseline to peak of induction. Glutamine is derived from proteolysis of host tissues, and serves as a precursor for glutamate (Nurjhan et al., 1995). Additionally, reduced levels of glutamate will drive the reaction of glutamine to glutamate via the enzyme glutaminase (glutamine and glutamate metabolism sub-pathway, Figure 4a) that releases additional ammonia that will serve to raise the pH of the environment. In fact, periodontitis is associated with a rise in pH above neutrality and increased probing depth and inflammation have been correlated with increased alkalization (Bickel & Cimasoni, 1995; Holt & Ebersole, 2005).

Amino acids histidine and histidine metabolites trans- and cis-urocanate have been shown to have anti-inflammatory activities (Hasegawa et al., 2012). In addition, trans-urocanate can be further metabolized to glutamate and thus serve as a potential energy source for bacteria. Mean changes of histidine were statistically significantly decreased from baseline to peak of induction

25

while changes in trans-urocanate and cis-urocanate demonstrated trending decreases from peak of induction to peak of resolution. Lower levels of histidine and the urocanates at peak of induction and peak of resolution could have negative consequences on oral health due to their anti-inflammatory properties. Glutamate and histidine share several metabolic pathways including the histidine metabolism sub-pathway and the purine metabolism sub-pathway. Statistically significant decreases in mean levels of these two metabolites at peak of induction may suggest an important role of these two pathways in the initiation of periodontal inflammation. Like the glutamine and glutamate metabolism sub-pathway, the reaction from histidine to the urocanates increases ammonia. This pathway may also serve to raise the pH of the environment.

Additionally, mean changes of 5-oxoproline were statistically significantly decreased from baseline to peak of induction ($q = 0.02$). 5-oxoproline is hydrolyzed to glutamate by 5-oxoprolinase (Figure 4d). Additionally, glutamine, which shares multiple metabolic pathways with glutamate, demonstrated a trending decrease from baseline to peak of induction. The finding that 5-oxoproline was statistically significantly decreased from baseline to peak of induction and glutamine demonstrated a trending decrease from baseline to peak of induction further strengthens the suggestion that glutamate is an important energy source for bacterial populations in periodontal inflammation. By-products of the glutathione metabolism sub-pathway are energy by-products including ADP and NADPH which serve to alter the redox potential of the local environment (Main et al., 2012). Additionally, conversion of glutamate to glutathione results in oxidation of reactive oxygen species which has been implicated in several other diseases such as cardiovascular disease, ischemic-reperfusion injury, diabetes, hypertension and inflammatory disease (Chae et al., 2013; Ren, Zhang, Cui, & Mu, 2013). Paradoxically,

26

Barnes et al. (2013) demonstrated elevated 5-oxoproline, glutamate, cysteine, γ-glutamyl-AA, glutathione disulfide (oxidized) and cysteine-glutathione disulfide (components of glutathione metabolism) in saliva when comparing diabetic and non-diabetic subjects with healthy periodontium, gingivitis and periodontitis (Barnes et al., 2013, March). However, this effect was more pronounced in diabetic subjects.

Erythronate is an organic acid present in healthy adults and children in the aqueous humor of the eye, connective tissue, urine, plasma, cerebrospinal fluid and synovial fluid (Harding, Hassett, Rixon, Bron, & Harvey, 1999). Erythronate is formed when N-Acetyl-D-glucosamine is oxidized (Jahn, Baynes, & Spiteller, 1999). N-Acetyl-D-glucosamine is a component of hyaluronic acid which is glycosaminoglycan found in human connective tissue inclusive of the periodontium (Sukumar & Drizhal, 2007). Erythronate is also derived from degradation of ascorbic acid, which is an anti-oxidant (Harding et al., 1999). Mean changes of erythronate were statistically significantly decreased from baseline to peak of induction ($q <$ 0.05). To our knowledge, erythronate has not been investigated in gingivitis and periodontitis. Barnes et al. (2009) reported a statistically significant decrease in ascorbic acid found in the GCF of diseased sites. Since oxidative stress has been implicated in the pathogenesis of periodontitis (Galli, Passeri, & Macaluso, 2011), decreased levels of anti-oxidants such as ascorbic acid would be expected. It is possible that decreased levels of erythronate detected in this study at peak of induction reflects an enhanced oxidative state.

BCAAs isoleucine and valine showed trending, although not statistically significant, decreases at peak of induction as compared to baseline in the BGI-H category (unadjusted $p <$ 0.05). BCAAs are among the most common amino acids metabolized by oral bacteria. Other mediators of the valine, leucine and isoleucine metabolism pathway, including 3-

hydrohyisobutyrate and citramalate, showed trending changes in the BGI-H category (unadjusted $p < 0.05$). The lack of similar changes in the other four disease states could reflect a pre-existing hyper-inflammatory state.

Tyrosine is an essential amino acid that is involved in several functions including neurotransmitter and hormone synthesis and is rapidly metabolized (Rasmussen, Ishizuka, Quigley, & Yen, 1983). It is involved in a number of pathways including phenylalanine and tyrosine metabolism sub-pathways. Mean changes of tyrosine were statistically significantly decreased from baseline to peak of induction ($q < 0.05$) which reinforces the suggestion that gingival bacterial populations rely on amino acid catabolism for energy. Trending decreases were seen among several metabolites in the phenyalanine metabolism sub-pathway including P-cresol sulfate and phenylacetate. These results are in contrast with Barnes et al. (2011) who demonstrated no significant difference in tyrosine and a trending increase in P-cresol sulfate in subjects with periodontitis as compared to healthy subjects (Barnes et al., 2011). One must be cautious in comparing these results since Barnes et al.(2011) reports cross-sectional data while this study was longitudinal.

Our data indicate that some changes in clinical indices co-vary with changes in metabolites in BGI categories. Changes in BOP within the BGI-P1 category demonstrate the strongest correlation with two metabolites, 3-aminoisobutyrate and 1,3-diaminopropane, from the nucleotide and amino acid super-family, respectively. To our knowledge, aminoisobutyrate and 1,3-diaminopropane have not been investigated in gingivitis and periodontitis.

3-aminoisobutyrate is the end-product of pyramidine metabolism and originates from catabolism of thymine and valine. Studies have demonstrated persistently elevated levels of 3-aminoisobutyrate in patients with deficiency of R (-) -b- aminoisobutyrate-pyruvate

aminotransferase and transiently elevated levels of 3-aminoisobutyrate in lead poisoning, starvation, total body irradiation, malignancies, neurological disorders and developmental delay (van Gennip et al., 1987). Elevated levels have been suggested to contribute to neurological and developmental problems since it is a structural analog for gamma-aminobutyric acid and glycine which are two major inhibitory neurotransmittors in the central nervous system (van Kuilenburg et al., 2004). 1,3-diaminopropane is a member of both the arginine and proline and beta-alanine metabolic pathways. Abnormal levels found in breast cancer and leukemia (Byun et al., 2008; Lee et al., 1998)**.**

Strong positive correlations between changes in BOP and glutamate and glutamine at peak of induction in the BGI-H category contradict previously reported data in this manuscript. Recall that when samples were not stratified by BGI category, mean levels of glutamate were statistically significantly decreased from baseline to peak of induction and mean levels of glutamine demonstrated a trending decrease from baseline to peak of induction. Since BGI-G, P1, P2 and P3 categories have an increased clinical inflammatory status, slight increases in glutamate and glutamine in the BGI-H group may have been masked when all subjects were analyzed together. It would be interesting to investigate changes in clinical indices and changes in glutamate and glutamine using the SIBO model with larger sample sizes to see if the correlation is stronger. Similarly, strong positive correlations between various clinical indices and threonine, histidine and 5-oxoproline in various BGI categories contradict previously reported data in this manuscript which may be related to the relatively small sample size.

Section 3.5: Conclusion

Among the 281 biochemicals identified in the saliva from the subjects in this study, only eight metabolites demonstrated a statistically significant change (applying FDR, $q < 0.05$) from baseline to peak of induction when samples were not stratified by BGI category. When samples were stratified by BGI category, no statistically significant changes were noted (applying FDR, $q < 0.05$). Trending changes were noted in each BGI category (unadjusted p-values). Our data indicate that two metabolites demonstrate very strong correlation with changes in BOP (applying FDR, $q < 0.05$) in the BGI-P1 category. This finding warrants further investigation. The relatively low sample number per group in conjunction with the normal high level of variability in human subjects likely contributed to the low number of observed differences achieving statistical significance. Trending changes observed in this study may provide an avenue for future investigation with larger sample sizes.

TABLE 1.1: DEMOGRAPHICS BY BGI CATEGORY (N = 50)

Characteristic (All)	BGI-H	BGI-G	BGI-P1	BGI-P2	BGI-P3	*p*-value*
Sex						0.21
Female	7 (21.2%)	7 (21.2%)	9 (27.3%)	6 (18.2%)	4 (12.1%)	
Male	3 (17.7%)	3 (17.7%)	1 (5.9%)	4 (23.5%)	6 (35.3%)	
Race						0.87
African American	6 (23.1%)	6 (23.1%)	5 (19.2%)	6 (23.1%)	3 (11.5%)	
Caucasian	3 (15.0%)	3 (15.0%)	4 (20.0%)	4 (20.0%)	6 (30.0%)	
Other	1 (25.0%)	1 (25.0%)	1 (25.0%)	0 (0.0%)	1 (25.0%)	
Diabetes						0.40
Yes	0 (0.0%)	1 (100%)	0 (0.0%)	0 (0.0%)	0 (0.0%)	
No	10 (20.4%)	9 (18.4%)	10 (20.4%)	10 (20.4%)	10 (20.4%)	
Former Smoker						0.054
Yes	0 (0.0%)	2 (28.5%)	4 (57.1%)	1 (14.3%)	0 (0.0%)	
No	10 (23.3%)	8 (18.6%)	6 (14.0%)	9 (20.8%)	10 (23.3%)	
Mean Age (StdDev)	26.4 (4.9)	30.9 (8.3)	38.0 (11.9)	32.4 (7.0)	27.5 (9.3)	0.03
Mean BMI (StdDev)	23.8 (4.5)	31.4 (7.2)	28.5 (7.0)	29.2 (5.2)	25.9 (6.8)	0.08

*Chi-squared test (χ^2) used to determine statistical significance between categorical variables. General linear models used to determine statistical significance between means.

TABLE 1.2: BASELINE CLINICAL INDICES BY BGI CATEGORY (N = 50)

Clinical index	BGI-H	BGI-G	BGI-P1	BGI-P2	BGI-P3
PI	0.57 (0.11)	0.79 (0.09)	0.58 (0.13)	1.09 (0.08)	1.27 (0.14)
GI	0.71 (0.11)	1.00 (0.07)	0.77 (0.09)	1.21 (0.04)	1.38 (0.09)
BOP	7.53 (1.81)	33.5 (6.12)	8.78 (1.40)	37.3 (4.61)	64.6 (2.97)
PD	1.80 (0.05)	2.09 (0.07)	1.95 (0.09)	2.19 (0.06)	2.23 (0.07)
CAL	0.90 (0.05)	1.00 (0.05)	0.99 (0.06)	0.94 (0.04)	1.07 (0.09)

Mean clinical values (standard error) for stent side at screening (Day -7).

TABLE 2.1 – MEAN CLINICAL CHANGES DURING INDUCTION AND RESOLUTION OF EXPERIMENTAL SIBO (N = 50)

	Baseline	**Stent in place**			**Resolution**	
		Day 7	**Day 14**	**Day 21**	**Day 35**	**Day 49**
Mean PI	0.75 (0.06)	1.39 (0.06)†	1.49 (0.06)†	1.54 (0.06)†	0.76 (0.07)†	0.76 (0.07)†
Mean GI	0.86 (0.04)	1.05 (0.04)**	1.16 (0.04)†	1.19 (0.04)†	0.84 (0.04)†	0.88 (0.04)†
BOP	28.6 (2.48)	37.3 (2.51)*	46.5 (2.48)†	48.0 (2.48)†	26.9 (2.62)†	30.6 (2.64)†
Mean PD	2.14 (0.04)	2.15 (0.05)	2.18 (0.04)	2.20 (0.04)	2.07 (0.05)*	2.18 (0.05)
Mean AL	1.09 (0.04)	1.05 (0.04)	1.04 (0.04)	1.08 (0.04)	1.00 (0.04)	1.07 (0.04)

Mean clinical values (standard error) for stent side. General linear model used to compare Days 7–21 with baseline and Days 35 and 49 with Day 21; *p*-value: *$p<0.05$, **$p<0.001$, $\dagger p<0.0001$.

TABLE 2.2 – MEAN CLINICAL CHANGES DURING INDUCTION AND RESOLUTION OF EXPERIMENTAL SIBO BY BGI CATEGORY (N = 50 TOTAL; N = 10 PER BGI CATEGORY)

		Baseline	Stent in place			Resolution	
	BGI		Day 7	Day 14	Day 21	Day 35	Day 49
Mean PI	H	0.37 (0.14)	1.19 (0.14)†	1.35 (0.14)†	1.48 (0.14)†	0.71 (0.16)**	0.56 (0.16)†
	G	0.62 (0.11)	1.30 (0.11)†	1.28 (0.11)†	1.39 (0.11)†	0.62 (0.12)†	0.62 (0.13)†
	P1	0.76 (0.11)	1.56 (0.11)†	1.76 (0.11)†	1.50 (0.11)†	0.81 (0.11)†	0.93 (0.11)**
	P2	0.77 (0.11)	1.47 (0.11)†	1.46 (0.11)†	1.59 (0.11)†	0.68 (0.11)†	0.73 (0.11)†
	P3	1.21 (0.19)	1.46 (0.19)	1.62 (0.19)	1.73 (0.19)	0.96 (0.19)*	0.84 (0.19)*
Mean GI	H	0.50 (0.10)	0.91 (0.10)*	1.01 (0.10)**	1.01 (0.10)**	0.87 (0.12)	0.56 (0.12)*
	G	0.74 (0.07)	0.99 (0.07)*	1.15 (0.07)**	1.12 (0.07)**	0.83 (0.08)*	0.89 (0.08)*
	P1	0.86 (0.06)	1.06 (0.06)*	1.13 (0.06)*	1.12 (0.06)*	0.75 (0.06)†	0.97 (0.06)
	P2	1.00 (0.08)	1.18 (0.08)	1.24 (0.08)*	1.31 (0.08)*	0.76 (0.08)†	0.89 (0.08)**
	P3	1.19 (0.09)	1.13 (0.09)	1.27 (0.09)	1.38 (0.09)	1.02 (0.09)*	1.02 (0.09)*
BOP	H	14.1 (4.44)	28.9 (4.44)*	32.5 (4.44)*	35.1 (4.44)*	20.0 (5.30)*	24.3 (5.30)
	G	23.0 (4.45)	31.7 (4.45)	41.8 (4.45)*	47.8 (4.45)**	26.9 (4.98)*	34.8 (5.31)
	P1	21.5 (4.84)	31.8 (4.84)	49.0 (4.84)**	47.2 (4.84)**	26.3 (4.84)*	29.6 (4.84)*
	P2	34.5 (4.80)	48.7 (5.06)*	51.3 (4.80)*	53.7 (4.80)*	20.0 (4.80)†	30.1 (4.80)*
	P3	49.7 (6.48)	46.6 (6.48)	57.6 (6.48)	56.1 (6.48)	39.4 (6.48)	33.7 (6.48)*
Mean PD	H	1.94 (0.11)	2.00 (0.11)	2.05 (0.11)	2.01 (0.11)	1.82 (0.13)	1.98 (0.13)
	G	2.22 (0.12)	2.19 (0.12)	2.27 (0.12)	2.22 (0.12)	2.10 (0.14)	2.09 (0.15)
	P1	2.05 (0.09)	2.11 (0.09)	2.17 (0.09)	2.28 (0.09)	2.24 (0.09)	2.16 (0.09)
	P2	2.16 (0.07)	2.18 (0.07)	2.15 (0.07)	2.19 (0.07)	1.96 (0.07)*	2.14 (0.07)
	P3	2.33 (0.09)	2.28 (0.09)	2.26 (0.09)	2.29 (0.09)	2.16 (0.09)	2.46 (0.09)
Mean AL	H	1.06 (0.09)	1.05 (0.09)	1.00 (0.09)	1.04 (0.09)	0.84 (0.11)	0.99 (0.11)
	G	1.09 (0.08)	0.99 (0.08)	1.08 (0.08)	1.04 (0.08)	0.94 (0.09)	0.97 (0.09)
	P1	1.16 (0.08)	1.05 (0.08)	0.95 (0.08)	1.14 (0.08)	1.03 (0.08)	0.93 (0.08)
	P2	1.08 (0.06)	1.00 (0.06)	1.11 (0.06)	0.98 (0.06)	1.05 (0.06)	1.06 (0.06)
	P3	1.06 (0.08)	1.17 (0.08)	1.07 (0.08)	1.21 (0.08)	1.07 (0.08)	1.34 (0.08)

Mean clinical value (standard error) for stent side. General linear model used to compare Days 7–21 with baseline and Days 35 and 49 with Day 21; *p*-value: *$p<0.05$, **$p<0.001$, †$p<0.0001$.

TABLE 3.1 – MEAN METABOLITE LEVELS DURING INDUCTION AND RESOLUTION
OF EXPERIMENTAL SIBO (N = 50)

Metabolite	Super-pathway	Sub-pathway	Baseline	Day 21	Day 49	q-value
Threonine	Amino acid	Glycine, serine and threonine metabolism	0.40	0.29	0.32	<0.01
N-acetylserine	Amino acid	Glycine, serine and threonine metabolism	0.31	0.23	0.25	0.02
Serine	Amino acid	Glycine, serine and threonine metabolism	0.40	0.30	0.31	0.02
5-oxoproline	Amino acid	Glutathione metabolism	0.36	0.27	0.32	0.02
Histidine	Amino acid	Histidine metabolism	0.35	0.29	0.32	0.03
Glutamate	Amino acid	Glutamate metabolism	0.36	0.30	0.31	0.03
Erythronate	Carbohydrate	Aminosugars metabolism	0.34	0.29	0.32	<0.05
Tyrosine	Amino acid	Phenylalanine & tyrosine metabolism	0.34	0.29	0.30	<0.05

Log of mean metabolites reported as raw concentrations. FDR-adjusted p-values (q-values) were
used to compare peak of induction (Day 21) with baseline, only metabolites with $q < 0.05$ were
reported. FDR was used to compare peak of resolution (Day 49) with peak of induction (Day
21); no metabolites with $q < 0.05$ were noted (data not reported).

TABLE 3.2 – TOP FIVE MEAN METABOLITE LEVELS DURING INDUCTION OF EXPERIMENTAL SIBO BY BGI CATEGORY (N = 50; N = 10 PER BGI CATEGORY)

BGI	Metabolite	Super-pathway	Baseline	Day 21	Day 49	p-value*	q-value[†]
H	Panose	Carbohydrate	0.38	0.25	0.28	**<0.01**	0.13
	Glycyltyrosine	Peptide	0.45	0.27	0.34	**<0.01**	0.13
	Isobar: dihydrocaffeate, 3,4-dihydroxycinnamate	Xenobiotics	0.40	0.30	0.46	**<0.01**	0.13
	Pantothenate	Cofactors and vitamins	0.38	0.27	0.32	**<0.01**	0.13
	5,6-dihydrothymine	Nucleotide	0.39	0.27	0.35	**<0.01**	0.13
G	Homoserine	Amino acid	0.33	0.26	0.25	**0.02**	0.92
	Hippurate	Xenobiotics	0.30	0.39	0.29	**0.03**	0.92
	Glycylleucine	Peptide	0.27	0.34	0.30	**0.03**	0.92
	Phosphoethanolamine	Lipid	0.31	0.37	0.28	0.13	0.92
	Adenine	Nucleotide	0.22	0.31	0.38	0.19	0.92
P1	2-hydroxy-3-methylvalerate	Amino acid	0.29	0.22	0.36	**0.02**	0.92
	Creatine	Amino acid	0.15	0.35	0.26	**0.02**	0.92
	5-oxoproline	Amino acid	0.39	0.29	0.28	**0.03**	0.92
	Thymine	Nucleotide	0.30	0.19	0.20	**0.04**	0.92
	3-aminoisobutyrate	Nucleotide	0.13	0.22	0.17	**0.04**	0.92
P2	Alpha-tocopherol	Cofactors and vitamins	0.41	0.26	0.44	**<0.01**	0.23
	Carnitine	Lipid	0.35	0.16	0.23	**<0.00**	0.23
	2-aminophenol	Amino acid	0.28	0.18	0.22	**0.01**	0.32
	Glycylproline	Peptide	0.33	0.22	0.29	**0.01**	0.32
	Guanine	Nucleotide	0.35	0.27	0.28	**0.01**	0.32
P3	Glucose-6-phosphate	Carbohydrate	0.46	0.32	0.33	**0.02**	0.76
	Arginylleucine	Peptide	0.39	0.31	0.29	**0.04**	0.76
	3-hydroxyisobutyrate	Amino acid	0.36	0.28	0.33	**0.04**	0.76
	Glycerate	Carbohydrate	0.27	0.18	0.26	**0.04**	0.76
	Acetylcarnitine	Lipid	0.32	0.27	0.29	**0.04**	0.76

Log of mean metabolites reported as raw concentrations. * unadjusted p-values used to compare peak of induction (Day 21) with baseline. †FDR-adjusted p-values; no metabolites with $q < 0.05$ were noted. **Red values** indicated decreased metabolite levels from baseline to peak of induction (Day 21). **Blue values** indicated increased metabolite levels from baseline to peak of induction (Day 21).

TABLE 3.3 – TOP FIVE MEAN METABOLITE LEVELS DURING RESOLUTION OF EXPERIMENTAL SIBO BY BGI CATEGORY (N = 50; N = 10 PER BGI CATEGORY)

BGI	Metabolite	Super-pathway	Baseline	Day 21	Day 49	p-value*	q-value[†]
H	serylleucine	Peptide	0.29	0.18	0.30	**<0.01**	0.62
	Isobar: dihydrocaffeate, 3,4-dihydroxycinnamate	Xenobiotics	0.40	0.30	0.46	**0.01**	0.81
	citramalate	Amino acid	0.35	0.24	0.31	**0.01**	0.81
	isoleucine	Amino acid	0.38	0.28	0.36	**0.02**	0.81
	beta-alanine	Amino acid	0.23	0.09	0.21	**0.02**	0.81
G	phosphoethanolamine	Lipid	0.31	0.37	0.28	**0.00**	0.08
	adenine	Nucleotide	0.22	0.31	0.38	**0.01**	0.97
	linolenate [alpha or gamma; (18:3n3 or 6)]	Lipid	0.24	0.19	0.11	**0.02**	0.97
	hippurate	Xenobiotics	0.30	0.39	0.29	**0.03**	0.97
	2-aminophenol	Amino acid	0.32	0.31	0.23	**0.03**	0.97
P1	hypotaurine	Amino acid	0.21	0.24	0.15	**0.01**	0.54
	daidzein	Xenobiotics	0.25	0.38	0.23	**0.01**	0.54
	choline phosphate	Lipid	0.32	0.34	0.22	**0.01**	0.54
	alanylalanine	Peptide	0.30	0.29	0.14	**0.01**	0.54
	erythritol	Xenobiotics	0.25	0.33	0.23	**0.02**	0.54
P2	alpha-tocopherol	Cofactors and vitamins	0.41	0.26	0.44	**0.01**	0.76
	hypoxanthine	Nucleotide	0.44	0.34	0.51	**0.01**	0.76
	lysine	Amino acid	0.47	0.37	0.52	**0.01**	0.76
	uracil	Nucleotide	0.35	0.35	0.45	**0.01**	0.76
	pipecolate	Amino acid	0.17	0.19	0.28	**0.03**	0.76
P3	pinitol	Lipid	0.19	0.13	0.24	**0.01**	0.56
	5-oxoproline	Amino acid	0.43	0.28	0.36	**0.01**	0.56
	sorbitol	Carbohydrate	0.35	0.24	0.40	**0.01**	0.56
	2-methylbutyroylcarnitine	Amino acid	0.34	0.19	0.32	**0.01**	0.56
	trans-4-hydroxyproline	Amino acid	0.39	0.34	0.40	**0.01**	0.56

Log of mean metabolites reported as raw concentrations. * unadjusted p-values used to compare peak of induction (Day 21) with peak of resolution. †FDR-adjusted p-values; no metabolites with $q < 0.05$ were noted. **Red values** indicated decreased metabolite levels from peak of induction (Day 21) to peak of resolution (Day 49). **Blue values** indicated increased metabolite levels from peak of induction (Day 21) to peak of resolution (Day 49).

TABLE 3.4 – SUMMARY OF CHANGES OF METABOLITES FROM BIOCHEMICAL
PATHWAYS ALTERED BY EXPERIMENTAL SIBO

Biochemical pathway	Change from baseline to peak of induction
Glycine, serine and threonine metabolism	Down
Valine, leucine and isoleucine biosynthesis	Down
Glutamate metabolism	Down
Histidine metabolism	Down
Purine metabolism	Down
Glutathione metabolism	Down
Phenylalanine & tyrosine metabolism	Down

TABLE 4.1. MEAN CHANGES IN METABOLITES THAT CO-VARY WITH CHANGES IN CLINICAL INDICES AT PEAK OF INDUCTION (N = 50)

Clinical index	Metabolite	Super-pathway	Correlation Coefficient	*p*-value
PI	1,2-propanediol	Lipid	0.39	0.01
	1,3-diaminopropane	Amino acid	0.35	0.01
	1,5-anhydroglucitol	Carbohydrate	0.35	0.01
	1,6-anhydroglucose	Carbohydrate	0.34	0.02
	1-kestose	Xenobiotics	-0.33	0.02
	1-palmitoylplasmenylethanolamine	Lipid	0.32	0.02
	12-HETE	Lipid	0.32	0.02
	13-methylmyristic acid	Lipid	0.31	0.03
	2,3-dihydroxyisovalerate	Cofactors and vitamins	0.31	0.03
	2-aminoadipate	Amino acid	0.30	0.03
	2-aminobutyrate	Amino acid	0.30	0.03
	2-aminophenol	Amino acid	0.30	0.04
	2-ethylhexyl 4-methoxycinnamate	Xenobiotics	0.29	0.04
	2-hydroxy-3-methylvalerate	Amino acid	0.29	0.04
	2-hydroxybutyrate	Amino acid	-0.29	0.04
	2-hydroxyglutarate	Lipid	0.29	0.04
GI	4-hydroxy-3-methoxybenzyl alcohol	Xenobiotics	0.44	<0.01
	2-aminophenol	Amino acid	0.41	<0.01
	Cortisol	Lipid	0.32	0.02
BOP	1,2-propanediol	Lipid	0.48	<0.01
	3-aminoisobutyrate	Nucleotide	0.46	<0.01
	1,3-diaminopropane	Amino acid	0.43	<0.01
	2-methylbutyroylcarnitine	Amino acid	0.41	<0.01
	1-palmitoylplasmenylethanolamine	Lipid	0.34	0.01
	13-methylmyristic acid	Lipid	0.34	0.01
	Adenosine 2'-monophosphate	Nucleotide	-0.34	0.02
	12-HETE	Lipid	0.33	0.02
	4-acetamidophenol	Xenobiotics	0.33	0.02
	3-(2-pyrrolidinyl)pyridine	Xenobiotics	0.32	0.02
	1,5-anhydroglucitol	Carbohydrate	0.32	0.02
	2-hydroxyglutarate	Lipid	0.31	0.03

	2-hydroxy-3-methylvalerate	Amino acid	0.31	0.03
	Arginine	Amino acid	0.31	0.03
	Alpha-ketoglutarate	Energy	0.31	0.03
	3-dehydrocarnitine	Lipid	0.31	0.03
	Cyclo(phe-pro)	Peptide	0.30	0.03
	1,6-anhydroglucose	Carbohydrate	0.30	0.03
	2-aminoadipate	Amino acid	0.30	0.03
	Arachidonate	Lipid	0.30	0.04
	2-aminobutyrate	Amino acid	0.29	0.04
	Hypotaurine	Amino acid	0.29	0.04
	Diphenhydramine	Xenobiotics	0.28	0.05
	Hydrochlorothiazide	Xenobiotics	0.28	0.05
PD	Epicatechin	Xenobiotics	-0.40	<0.01
	Beta-alanine	Amino acid	0.38	0.01
	N-acetylgalactosamine	Carbohydrate	-0.38	0.01
	3-(4-hydroxyphenyl)lactate	Amino acid	-0.38	0.01
	3-phenylpropionate (hydrocinnamate)	Amino acid	-0.38	0.01
	Pipecolate	Amino acid	-0.37	0.01
	Glycerol	Lipid	-0.34	0.01
	Carnosine	Peptide	-0.34	0.02
	Cortisol	Lipid	-0.33	0.02
	5-aminovalerate	Amino acid	0.33	0.02
	Citrulline	Amino acid	-0.33	0.02
	Glycerate	Carbohydrate	-0.32	0.02
	Isovalerate	Lipid	-0.32	0.03
	Aspartate	Amino acid	0.31	0.03
	3-(4-hydroxyphenyl)propionate	Amino acid	-0.29	0.04
	2-hydroxybutyrate	Amino acid	0.28	0.05
CAL	Mannitol	Carbohydrate	-0.48	<0.01
	3-methylxanthine	Xenobiotics	-0.44	<0.01
	Dihomo-linolenate	Lipid	-0.44	<0.01
	Allantoin	Nucleotide	-0.42	<0.01
	3-phenylpropionate (hydrocinnamate)	Amino acid	-0.42	<0.01
	Fructose	Carbohydrate	-0.41	<0.01
	2-aminophenol	Amino acid	-0.41	<0.01

Beta-hydroxyisovalerate	Amino acid	-0.41	<0.01
Pipecolate	Amino acid	-0.39	0.01
Malate	Energy	-0.39	0.01
Guanosine	Nucleotide	-0.36	0.01
N-acetylgalactosamine	Carbohydrate	-0.35	0.01
Ribitol	Carbohydrate	-0.34	0.01
Glycine	Amino acid	-0.34	0.02
Phosphoenolpyruvate	Carbohydrate	0.33	0.02
Cyclo(phe-pro)	Peptide	-0.33	0.02
N-carbamoylaspartate	Amino acid	-0.32	0.03
Lactate	Carbohydrate	-0.32	0.03
Threonylphenylalanine	Peptide	0.32	0.03
Caffeate	Xenobiotics	0.31	0.03
Carnitine	Lipid	-0.31	0.03
Taurine	Amino acid	-0.30	0.03
Cortisone	Lipid	-0.30	0.03
Citrulline	Amino acid	-0.30	0.04
Cortisol	Lipid	-0.30	0.04
Guanine	Nucleotide	-0.29	0.04
Glycerate	Carbohydrate	-0.29	0.04
2-hydroxybutyrate	Amino acid	0.29	0.04
Phenylalanylleucine	Peptide	0.28	0.05
Isovalerylcarnitine	Amino acid	0.28	0.05

Correlation coefficients were evaluated using covariance matrices to describe a correlation between mean changes in metabolites and changes in clinical indices at peak of induction (Day 21). Correlations with $p < 0.05$ are reported in this table. FDR was applied to data; no metabolites with $q < 0.05$ were noted (data not reported).
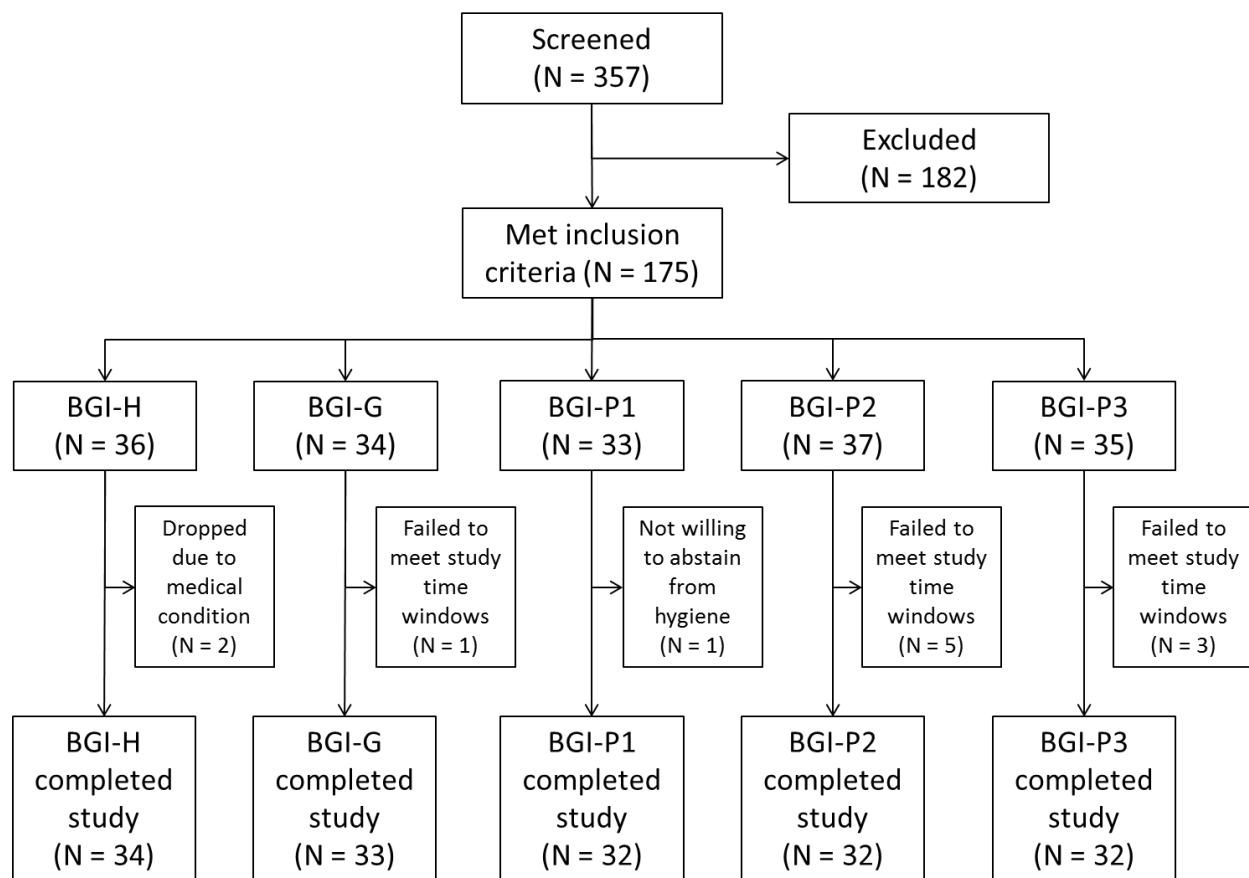
FIGURE 1 – FLOW OF PATIENT RECRUITMENT
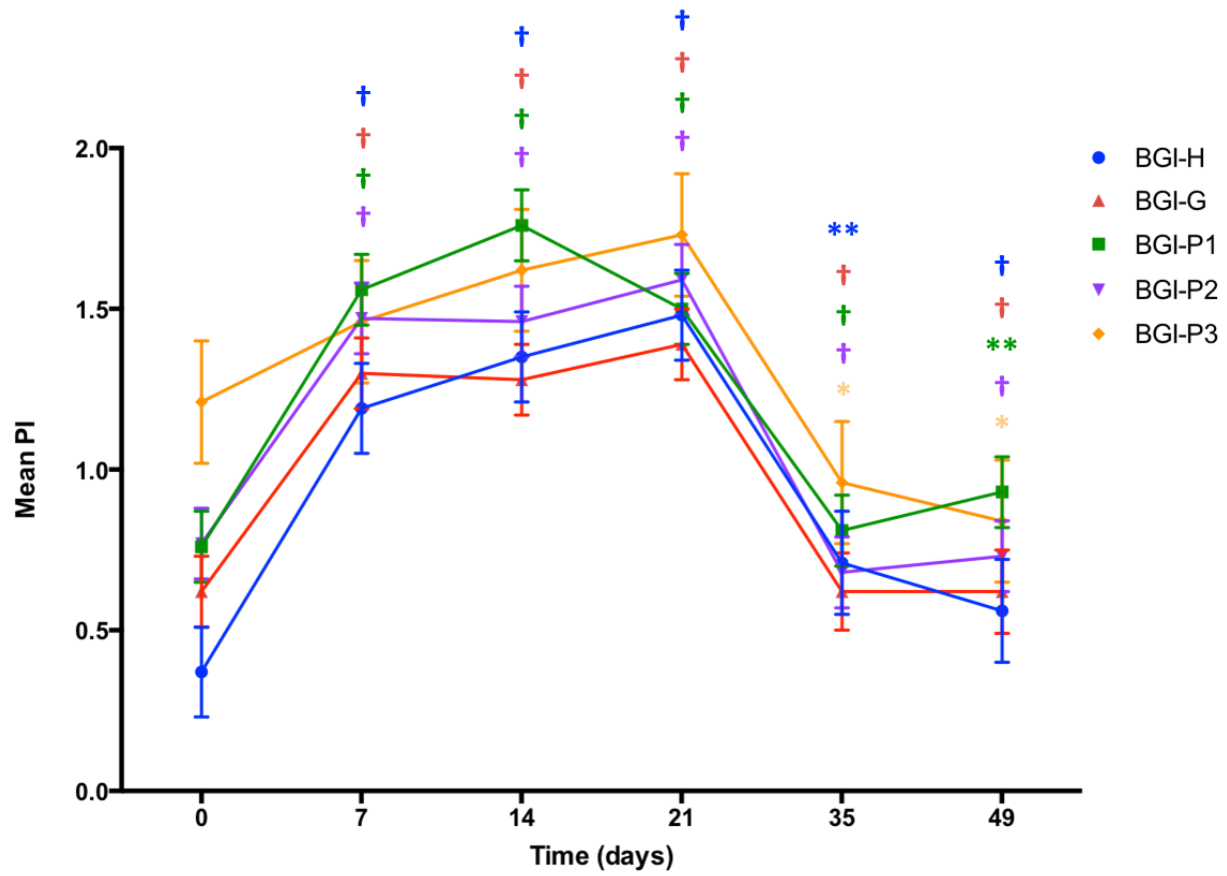
FIGURE 2.1 – MEAN PLAQUE INDEX DURING INDUCTION AND RESOLUTION OF
EXPERIMENTAL SIBO
Mean PI for stent side. General linear model used to compare Days 7–21 with baseline and Days
35 and 49 with Day 21; p-value: *$p<0.05$, **$p<0.001$, †$p<0.0001$.
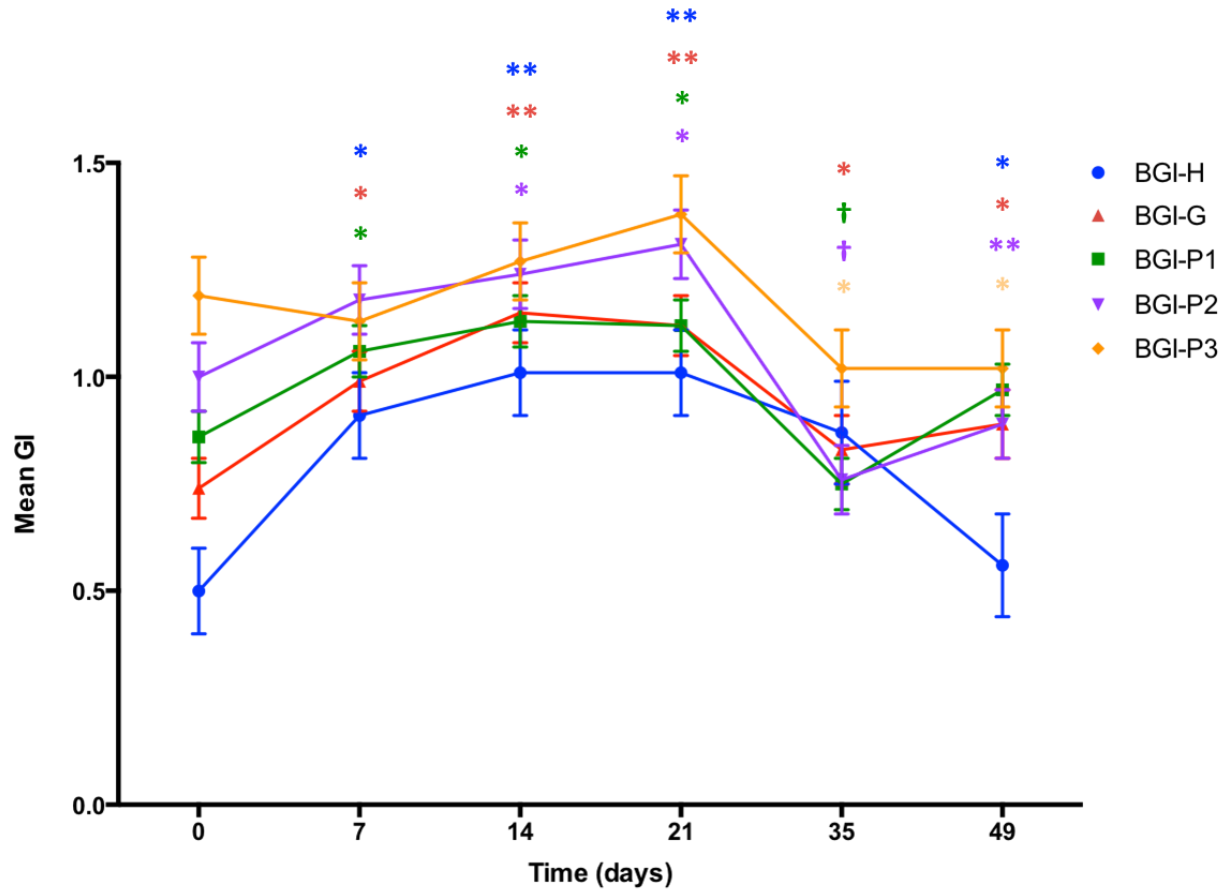
FIGURE 2.2 – MEAN GINGIVAL INDEX DURING INDUCTION AND RESOLUTION OF
EXPERIMENTAL SIBO
Mean GI for stent side. General linear model used to compare Days 7–21 with baseline and Days
35 and 49 with Day 21; *p*-value: *$p<0.05$, **$p<0.001$, †$p<0.0001$.
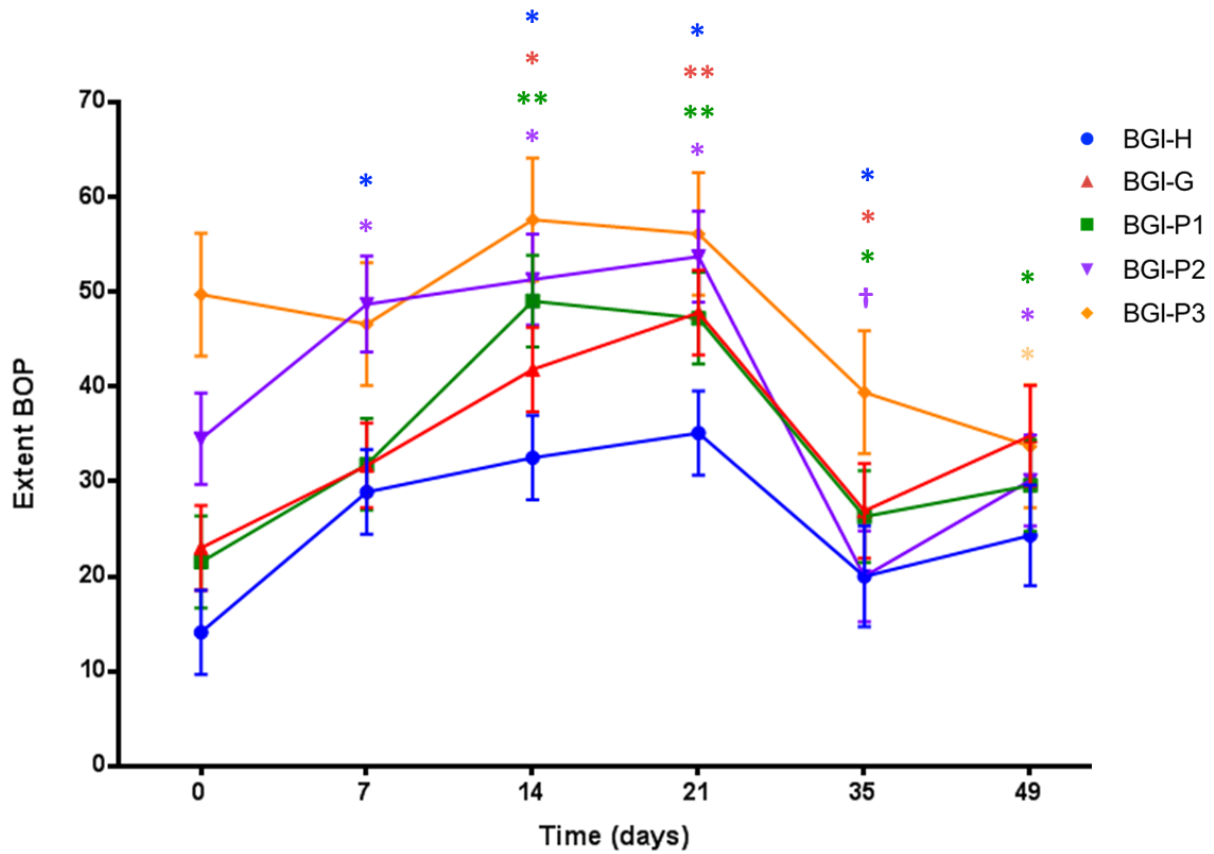
FIGURE 2.3 – EXTENT BLEEDING ON PROBING DURING INDUCTION AND RESOLUTION OF EXPERIMENTAL SIBO

Extent BOP for stent side. General linear model used to compare Days 7–21 with baseline and Days 35 and 49 with Day 21; p-value: $*p<0.05$, $**p<0.001$, $†p<0.0001$.
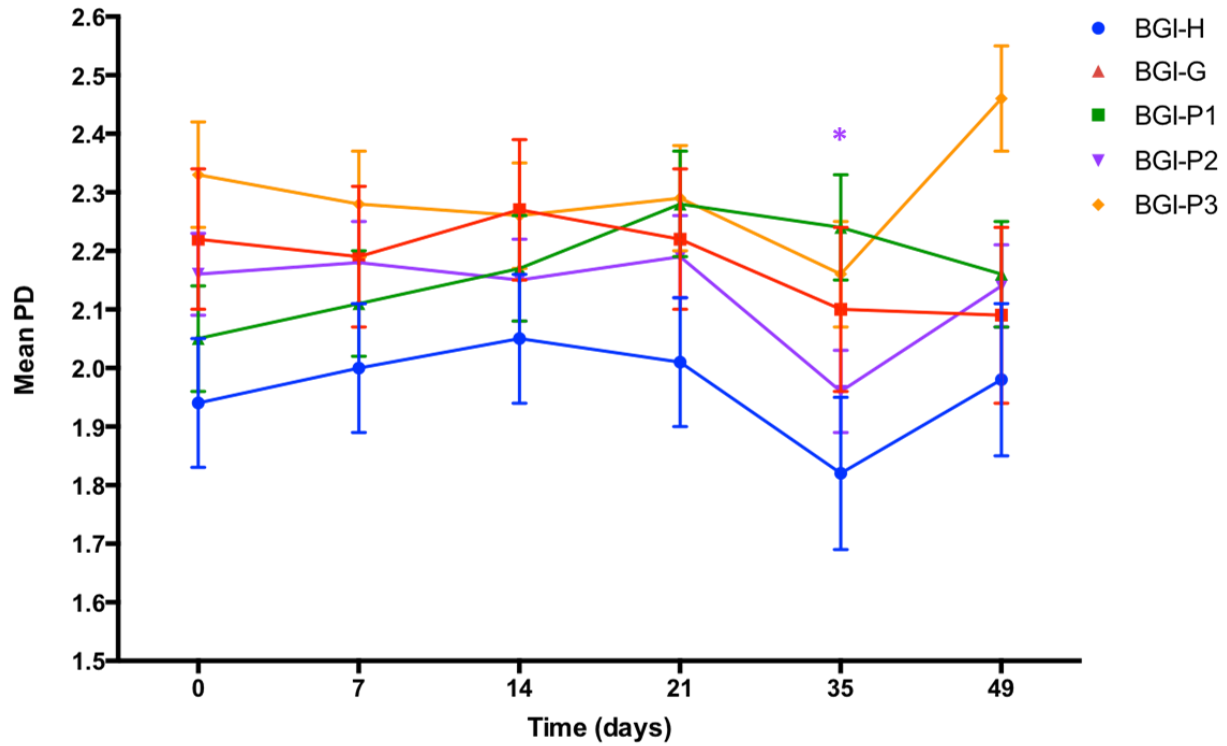
FIGURE 2.4 – MEAN PROBING DEPTH DURING INDUCTION AND RESOLUTION OF EXPERIMENTAL SIBO
Mean PD for stent side. General linear model used to compare Days 7–21 with baseline and Days 35 and 49 with Day 21; p-value: *$p<0.05$.
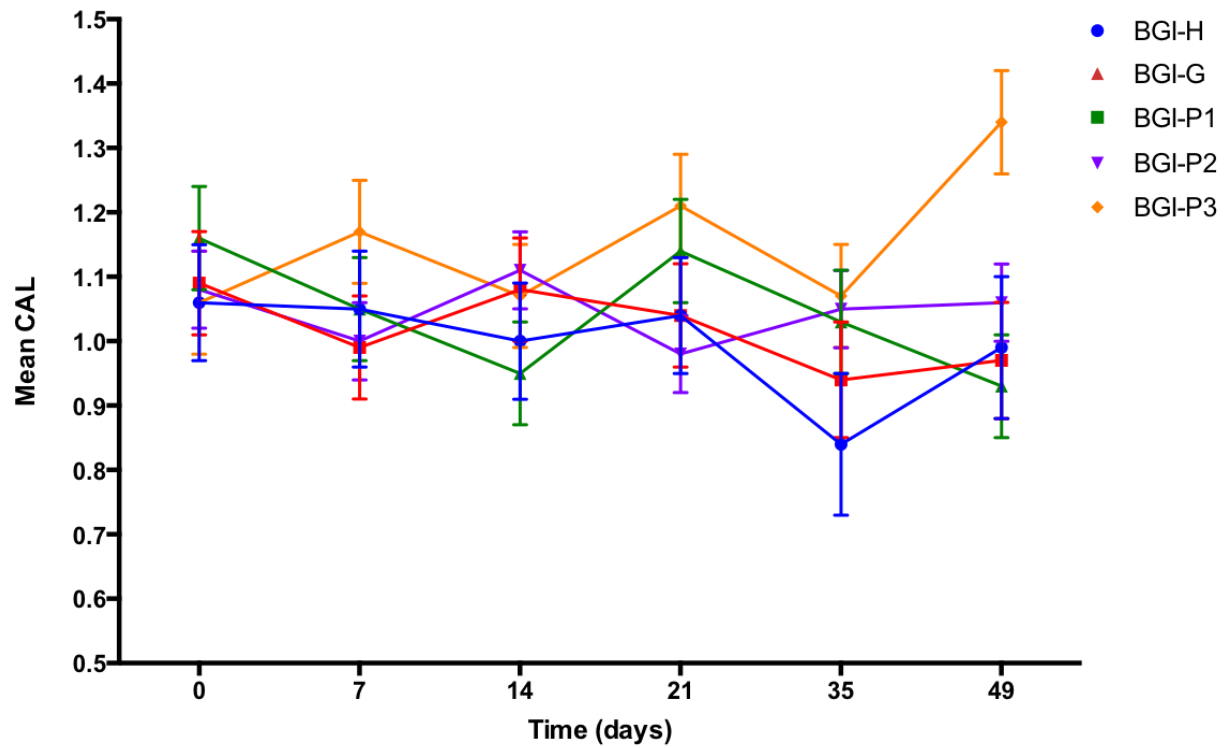
FIGURE 2.5 – MEAN CLINICAL ATTACHMENT LEVEL DURING INDUCTION AND RESOLUTION OF EXPERIMENTAL SIBO
Mean CAL for stent side. General linear model used to compare Days 7–21 with baseline and Days 35 and 49 with Day 21; no values reached statistical significance.

FIGURE 3 – OVERVIEW OF METABOLIC PATHWAYS

Metabolites that demonstrated statistically significant and trending changes in metabolites during experimental SIBO. **Red circles** indicate metabolites that demonstrated statistical significant decrease (applying FDR, $q < 0.05$) from baseline to peak of induction (Day 21) when samples were not stratified by BGI category (5-oxoproline, glutamate, histidine, serine, threonine, tyrosine). **Blue circles** indicate metabolites that demonstrated trending changes in each BGI category (unadjusted $p < 0.05$); 3-hydroxyisobutyrate demonstrated a trending decrease from baseline to peak of induction (Day 21) in BGI-H; 3-phenylpropionate demonstrated a trending increase from peak of induction (Day 21) to peak of resolution (Day 49) in BGI-P3; cis-urocanate demonstrated a trending decrease from baseline to peak of induction (Day 21) in BGI-P2 and a trending decrease from peak of induction (Day 21) to peak of resolution (Day 49) in BGI-P1; glutamine demonstrated a trending decrease from baseline to peak of induction (Day 21) when samples were not stratified by BGI category; glycine demonstrated a trending increase from baseline to peak of induction (Day 21) and decrease from peak of induction (Day 21) to peak of resolution (Day 49) in BGI-G; homoserine demonstrated a trending decrease from baseline to peak of induction (Day 21) in BGI-G; hypotaurine demonstrated a trending decrease from baseline to peak of induction (Day 21) in BGI-H; isoleucine demonstrated a trending decrease from baseline to peak of induction (Day 21) and trending increase from peak of induction (Day 21) to peak of resolution (Day 49) in BGI-H; o-acetylhomoserine demonstrated a trending increase from peak of induction (Day 21) to peak of resolution (Day 49) in BGI-P3; phenylacetate demonstrated a trending decrease from peak of induction (Day 21) to peak of resolution (Day 49) in BGI-H; phenyllactate demonstrated a trending decrease from baseline to peak of induction (Day 21) in BGI-H and trending increase from peak of induction (Day 21) to peak of resolution (Day 49) in BGI-P1; taurine demonstrated a trending decrease from peak of induction (Day 21) to peak of resolution (Day 49) in BGI-H; tyramine demonstrated a trending decrease from peak of induction (Day 21) to peak of resolution (Day 49) in BGI-P3; valine demonstrated a trending decrease from baseline to peak of induction (Day 21) in BGI-H.
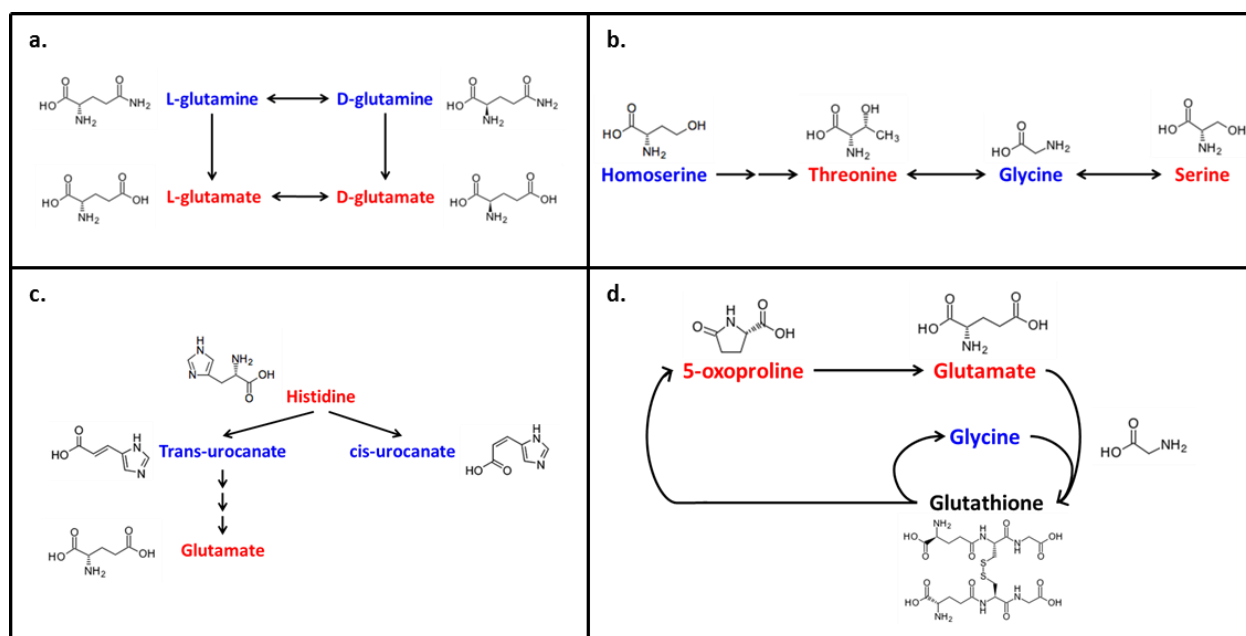
FIGURE 4 – SIMPLIFIED METABOLIC PATHWAYS
a) Glutamine and glutamate metabolism sub-pathway
b) Glycine, serine and threonine metabolism sub-pathway
c) Histidine metabolism sub-pathway
d) Glutathione metabolism sub-pathway

Red indicates metabolites that demonstrated statistical significant decrease (applying FDR, $q <$ 0.05) from baseline to peak of induction (Day 21) when samples were not stratified by BGI category. **Blue** indicate metabolites that demonstrated trending changes in each BGI category (unadjusted $p < 0.05$): cis-urocanate demonstrated a trending decrease from baseline to peak of induction (Day 21) in BGI-P2 and a trending decrease from peak of induction (Day 21) to peak of resolution (Day 49) in BGI-P1; glutamine demonstrated a trending decrease from baseline to peak of induction (Day 21) when samples were not stratified by BGI category; glycine demonstrated a trending increase from baseline to peak of induction (Day 21) and decrease from peak of induction (Day 21) to peak of resolution (Day 49) in BGI-G; homoserine demonstrated a trending decrease from baseline to peak of induction (Day 21) in BGI-G, trans-urocanate demonstrated a trending decrease from peak of induction (Day 21) to peak of resolution (Day 49) without stratifying by BGI category.

APPENDIX 3.1.1 – EXTENDED DETAILS OF METHODS

Analysis of salivary metabolome

Metabolomic analyses were conducted at Metabolon, Inc. (Durham, NC). Saliva samples were extracted and prepared for analysis using the automated MicroLab STAR® (Hamilton Robotics). The extraction steps were optimized for removal of protein and maximum recovery of small molecules including both aqueous and organic soluble metabolites (Lee, New, & Ong, 2003). Samples were placed briefly on a TurboVap® (Zymark) to remove the organic solvent. Each sample was then frozen and dried under vacuum. Samples were split into equal parts for analysis using GC/MS and LC/MS. Saliva samples were analyzed in duplicate from timepoints -14, 0, 21 and 49 days for each subject. Samples were subjected to both non-targeted and targeted analysis via LC/MS and GC/MS. Results were reported as raw concentrations of metabolites for five groups (BGI-H, BGI-G, BGI-P1, P2, and P3) at seven time points (Day -14, 0, 7, 14, 21, 35 and 49) which provided data at baseline, induction and resolution. All laboratory analyses were performed masked from sample, visit or patient information.

LC/MS

LC/MS was carried out using a Waters ACQUITY UPLC and a Thermo-Finnigan LTQ mass spectrometer, which consisted of an electrospray ionization source and linear ion-trap mass analyzer. The sample extract was split into two aliquots, dried, then reconstituted in acidic or basic LC-compatible solvents, each of which contained 11 or more injection standards at fixed concentrations. One aliquot was analyzed using acidic positive ion optimized conditions and the other using basic negative ion optimized conditions in two independent injections using separate dedicated columns. Extracts reconstituted in acidic conditions were gradient eluted using water

and methanol both containing 0.1% formic acid, while the basic extracts, which also used

water/methanol, contained 6.5mM ammonium bicarbonate. The MS analysis alternated between

MS and data-dependent MS2 scans using dynamic exclusion.

GC/MS

The samples destined for GC/MS analysis were re-dried under vacuum desiccation for a

minimum of 24 hours prior to being derivatized under dried nitrogen using bistrimethyl-silyl-

triflouroacetamide. The GC column was 5% phenyl and the temperature ramp is from 40° to

300°C in a 16 minute period. Samples were analyzed on a Thermo-Finnigan Trace DSQ fast-

scanning single-quadrupole mass spectrometer using electron impact ionization. The instrument

was tuned and calibrated for mass resolution and mass accuracy on a daily basis. The

information output from the raw data files was automatically extracted as discussed below.

Accurate mass determination and MS/MS fragmentation (LC/MS), (LC/MS/MS)

The LC/MS portion of the platform was based on a Waters ACQUITY UPLC and a

Thermo-Finnigan LTQ-FT mass spectrometer, which had a linear ion-trap (LIT) front end and a

Fourier transform ion cyclotron resonance (FT-ICR) mass spectrometer backend. For ions with

counts greater than two million, an accurate mass measurement could be performed. Accurate

mass measurements could be made on the parent ion as well as fragments. The typical mass error

was less than 5 ppm. Ions with less than two million counts require a greater amount of effort to

characterize. Fragmentation spectra (MS/MS) were typically generated in data dependent

manner, but if necessary, targeted MS/MS could be employed, such as in the case of lower level

signals.

Compound identification

Compounds were identified by comparison to library entries of purified standards or recurrent unknown entities. Identification of known chemical entities was based on comparison to metabolomic library entries of purified standards. The combination of chromatographic properties and mass spectra gave an indication of a match to the specific compound or an isobaric entity. Additional entities could be identified by virtue of their recurrent nature (both chromatographic and mass spectral). These compounds have the potential to be identified by future acquisition of a matching purified standard or by classical structural analysis.

Data normalization

For studies spanning multiple days, a data normalization step was performed to correct variation resulting from instrument inter-day tuning differences. Each compound was corrected in run-day blocks by registering the medians to equal one and normalizing each data point proportionately. For studies that did not require more than one day of analysis, no normalization was necessary.

Quality control

Instrument variability was determined by calculating the median RSD for the internal standards that were added to each sample prior to injection into the mass spectrometers. Also included were several technical replicate samples created from a homogeneous pool containing a small amount of all study samples ("Client Matrix"). Overall process variability was determined by calculating the median RSD for all endogenous metabolites (i.e., non-instrument standards) present in 100% of the Client Matrix samples, which are technical replicates of pooled client

samples. Values for instrument and process variability associated with these samples met Metabolon's acceptance criteria. Instrument variability for the internal standards had a median RSD of 5% and total process variability for the endogenous biochemicals had a median RSD of 11% (APPENDIX 3.1.2).

APPENDIX 3.1.2 - INSTRUMENT AND PROCESS VARIABILITY.

Quality control sample	Measurement	Median RSD
Internal standards	Instrument variability	5%
Endogenous biochemicals	Overall process variability	11%

Internal standards were added into each study sample prior to injection into the MS instrument. Endogenous biochemicals from client matrix samples were technical replicates created from a small portion of experimental samples.

APPENDIX 3.2 – MEAN METABOLITE LEVELS DURING INDUCTION AND
RESOLUTION OF EXPERIMENTAL SIBO BY BGI CATEGORY (N = 50; N = 10 PER BGI
CATEGORY)

BGI	Metabolite	Super-pathway	Baseline	Day 21	Day 49	*p*-value*	*p*-value[†]
H	Panose	Carbohydrate	0.38	0.25	0.28	<0.01	0.58
	Glycyltyrosine	Peptide	0.45	0.27	0.34	<0.01	0.25
	Isobar: dihydrocaffeate, 3,4-dihydroxycinnamate	Xenobiotics	0.40	0.30	0.46	<0.01	0.01
	Pantothenate	Cofactors and vitamins	0.38	0.27	0.32	<0.01	0.38
	5,6-dihydrothymine	Nucleotide	0.39	0.27	0.35	<0.01	0.13
	Hexaethylene glycol	Xenobiotics	0.37	0.26	0.29	<0.01	0.40
	Histidine	Amino acid	0.41	0.27	0.30	<0.01	0.48
	Deoxycarnitine	Lipid	0.41	0.28	0.34	<0.01	0.08
	Vanillate	Xenobiotics	0.29	0.21	0.24	<0.01	0.27
	Sucrose	Carbohydrate	0.25	0.19	0.21	<0.01	0.32
	Glycerol 3-phosphate	Lipid	0.33	0.20	0.30	<0.01	0.02
	Choline	Lipid	0.41	0.20	0.26	<0.01	0.42
	Glycylleucine	Peptide	0.36	0.25	0.30	<0.01	0.07
	3-(4-hydroxyphenyl)lactate	Amino acid	0.37	0.27	0.32	<0.01	0.08
	Uracil	Nucleotide	0.57	0.22	0.30	<0.01	0.23
	Thymine	Nucleotide	0.35	0.21	0.24	<0.01	0.35
	1,3-diaminopropane	Amino acid	0.53	0.25	0.36	<0.01	0.10
	Fructose	Carbohydrate	0.55	0.30	0.37	<0.01	0.37
	Glycine	Amino acid	0.44	0.27	0.35	0.01	0.04
	Valine	Amino acid	0.39	0.24	0.32	0.01	0.08
	Arginylleucine	Peptide	0.41	0.23	0.35	0.01	0.11
	Linolenate	Lipid	0.39	0.16	0.19	0.01	0.55
	2,3-dihydroxyisovalerate	Cofactors and vitamins	0.38	0.31	0.29	0.01	0.69
	Taurine	Amino acid	0.41	0.31	0.31	0.01	0.92
	Nicotinate	Cofactors and vitamins	0.39	0.30	0.32	0.02	0.54
	5-oxoproline	Amino acid	0.44	0.27	0.32	0.02	0.32
	Inosine	Nucleotide	0.40	0.25	0.33	0.02	0.11
	Serylleucine	Peptide	0.29	0.18	0.30	0.02	<0.01
	Theophylline	Xenobiotics	0.38	0.25	0.32	0.03	0.23
	1,2-propanediol	Lipid	0.40	0.16	0.29	0.03	0.24
	Cotinine	Xenobiotics	0.42	0.24	0.31	0.03	0.08
	Alpha-ketoglutarate	Energy	0.42	0.18	0.30	0.03	0.09
	Hypoxanthine	Nucleotide	0.40	0.28	0.32	0.03	0.49
	Agmatine	Amino acid	1.05	0.33	0.50	0.04	0.30
	Isoleucine	Amino acid	0.38	0.28	0.36	0.04	0.02

	Uridine	Nucleotide	0.41	0.30	0.38	**0.04**	0.06
	3-hydroxyisobutyrate	Amino acid	0.43	0.28	0.30	**0.04**	0.64
	Fumarate	Energy	0.30	0.18	0.20	**0.04**	0.69
	Citramalate	Amino acid	0.35	0.24	0.31	**0.04**	**0.01**
	5-aminovalerate	Amino acid	0.40	0.32	0.37	**0.04**	0.17
	Sedoheptulose-7-phosphate	Carbohydrate	0.43	0.28	0.32	**0.04**	0.17
	Phenyllactate	Amino acid	0.58	0.33	0.43	**0.04**	0.27
	Tryptophan betaine	Amino acid	0.25	0.15	0.16	**0.04**	0.97
	Tryptophan	Amino acid	0.37	0.24	0.30	**0.04**	0.21
	Arginylisoleucine	Peptide	0.42	0.26	0.31	**0.04**	0.58
	P-cresol sulfate	Amino acid	0.39	0.29	0.32	**0.04**	0.41
	Ricinoleic acid	Xenobiotics	0.31	0.25	0.32	**<0.05**	0.06
	Aspartate	Amino acid	0.33	0.20	0.27	**<0.05**	0.13
	Beta-alanine	Amino acid	0.23	0.09	0.21	0.11	**0.02**
	Phenylacetate	Amino acid	0.32	0.26	0.32	0.08	**0.02**
	Gallate	Xenobiotics	0.30	0.23	0.28	0.09	**0.04**
	3,4-dihydroxybenzoate	Xenobiotics	0.29	0.24	0.30	0.21	**0.04**
	Lactate	Carbohydrate	0.22	0.12	0.24	0.14	**0.04**
G	Homoserine	Amino acid	0.33	0.26	0.25	**0.02**	0.77
	Hippurate	Xenobiotics	0.30	0.39	0.29	**0.03**	**0.03**
	Glycylleucine	Peptide	0.27	0.34	0.30	**0.03**	0.12
	Phosphoethanolamine	Lipid	0.31	0.37	0.28	0.13	**<0.01**
	Adenine	Nucleotide	0.22	0.31	0.38	0.19	**0.01**
	Linolenate	Lipid	0.24	0.19	0.11	0.22	**0.02**
	2-aminophenol	Amino acid	0.32	0.31	0.23	0.79	**0.03**
	Glutamate	Amino acid	0.41	0.38	0.14	0.67	**0.04**
	3-(2-pyrrolidinyl)pyridine	Xenobiotics	0.38	0.34	0.25	0.49	**0.04**
	Trans-4-hydroxyproline	Amino acid	0.29	0.30	0.26	0.64	**<0.05**
	N-acetylputrescine	Amino acid	0.35	0.37	0.22	0.87	**<0.05**
P1	2-hydroxy-3-methylvalerate	Amino acid	0.29	0.22	0.36	**0.02**	**0.02**
	Creatine	Amino acid	0.15	0.35	0.26	**0.02**	0.21
	5-oxoproline	Amino acid	0.39	0.29	0.28	**0.03**	0.63
	Thymine	Nucleotide	0.30	0.19	0.20	**0.04**	0.82
	3-aminoisobutyrate	Nucleotide	0.13	0.22	0.17	**0.04**	0.22
	Epicatechin	Xenobiotics	0.18	0.10	0.32	**0.04**	**0.04**
	Erythritol	Xenobiotics	0.25	0.33	0.23	0.05	**0.02**
	Hypotaurine	Amino acid	0.21	0.24	0.15	0.52	**0.01**
	Daidzein	Xenobiotics	0.25	0.38	0.23	0.17	**0.01**
	Choline phosphate	Lipid	0.32	0.34	0.22	0.84	**0.01**
	Alanylalanine	Peptide	0.30	0.29	0.14	0.97	**0.01**
	Erythritol	Xenobiotics	0.25	0.33	0.23	0.05	**0.02**

	Metabolite	Category					
	Xanthine	Nucleotide	0.25	0.29	0.20	0.39	**0.02**
	Palmitoyl sphingomyelin	Lipid	0.38	0.26	0.55	0.16	**0.02**
	Anserine	Peptide	0.22	0.27	0.20	0.29	**0.02**
	Alpha-tocopherol	Cofactors and vitamins	0.23	0.26	0.17	0.58	**0.03**
	Beta-hydroxyisovalerate	Amino acid	0.23	0.26	0.17	0.69	**0.03**
	Erythronate	Carbohydrate	0.27	0.34	0.21	0.45	**0.03**
	Serylleucine	Peptide	0.23	0.24	0.18	0.69	**0.04**
	Cis-urocanate	Amino acid	0.29	0.28	0.23	0.70	**0.04**
	N-acetylmannosamine	Carbohydrate	0.28	0.27	0.23	0.83	**0.04**
	Nicotinate	Cofactors and vitamins	0.30	0.28	0.25	0.58	**0.04**
	Serylisoleucine	Peptide	0.32	0.34	0.19	0.70	**0.04**
	Nicotinamide	Cofactors and vitamins	0.16	0.18	0.12	0.64	**0.05**
	2,3-dihydroxyisovalerate	Cofactors and vitamins	0.27	0.34	0.26	0.18	**0.05**
	Scyllo-inositol	Lipid	0.26	0.32	0.26	0.17	**0.05**
	Phenyllactate	Amino acid	0.44	0.33	0.54	0.21	**0.05**
	Alpha-hydroxyisocaproate	Amino acid	0.15	0.20	0.13	0.38	**0.05**
	Deoxycarnitine	Lipid	0.35	0.33	0.40	0.42	**0.05**
P2	Alpha-tocopherol	Cofactors and vitamins	0.41	0.26	0.44	**<0.01**	**0.01**
	Carnitine	Lipid	0.35	0.16	0.23	**<0.00**	0.26
	2-aminophenol	Amino acid	0.28	0.18	0.22	**0.01**	0.28
	Glycylproline	Peptide	0.33	0.22	0.29	**0.01**	0.15
	Guanine	Nucleotide	0.35	0.27	0.28	**0.01**	0.96
	Isoleucylisoleucine	Peptide	0.17	0.24	0.18	**0.01**	0.21
	Tyrosylleucine	Peptide	0.37	0.27	0.37	**0.01**	0.11
	Isobar: dihydrocaffeate, 3,4-dihydroxycinnamate	Xenobiotics	0.43	0.29	0.33	**0.02**	0.69
	12-HETE	Lipid	0.28	0.14	0.23	**0.03**	0.07
	Cytidine diphosphate	Nucleotide	0.36	0.27	0.36	**0.03**	0.07
	Sorbitol	Carbohydrate	0.39	0.24	0.39	**0.03**	0.27
	Tryptophan betaine	Amino acid	0.29	0.23	0.31	**0.03**	0.07
	N-acetylmannosamine	Carbohydrate	0.32	0.24	0.25	**0.04**	0.53
	Glucuronate	Carbohydrate	0.33	0.26	0.32	**0.04**	0.17
	N-carbamoylaspartate	Amino acid	0.45	0.35	0.40	**<0.05**	0.36
	Cis-urocanate	Amino acid	0.33	0.18	0.28	**<0.05**	0.19
	Hypoxanthine	Nucleotide	0.44	0.34	0.51	0.14	**0.01**
	Lysine	Amino acid	0.47	0.37	0.52	0.12	**0.01**
	Uracil	Nucleotide	0.35	0.35	0.45	0.94	**0.01**
	Pipecolate	Amino acid	0.17	0.19	0.28	0.75	**0.03**
	4-methyl-2-oxopentanoate	Amino acid	0.27	0.26	0.19	0.86	**0.03**

	Metabolite	Class					
	N-acetylglycine	Amino acid	0.36	0.30	0.40	0.13	**0.04**
P3	Glucose-6-phosphate	Carbohydrate	0.46	0.32	0.33	**0.02**	0.87
	Arginylleucine	Peptide	0.39	0.31	0.29	**0.04**	0.60
	3-hydroxyisobutyrate	Amino acid	0.36	0.28	0.33	**0.04**	0.11
	Glycerate	Carbohydrate	0.27	0.18	0.26	**0.04**	0.06
	Acetylcarnitine	Lipid	0.32	0.27	0.29	**0.04**	0.29
	Deoxycarnitine	Lipid	0.35	0.25	0.30	**0.04**	0.18
	Malate	Energy	0.32	0.26	0.25	**0.04**	0.44
	Linolenate	Lipid	0.24	0.10	0.13	**0.04**	0.40
	Lignocerate	Lipid	0.38	0.31	0.35	**0.04**	0.10
	5-oxoproline	Amino acid	0.43	0.28	0.36	**<0.05**	**0.01**
	Pinitol	Lipid	0.19	0.13	0.24	0.38	**0.01**
	Sorbitol	Carbohydrate	0.35	0.24	0.40	0.26	**0.01**
	2-methylbutyroylcarnitine	Amino acid	0.34	0.19	0.32	0.09	**0.01**
	Trans-4-hydroxyproline	Amino acid	0.39	0.34	0.40	0.26	**0.01**
	Pseudoephedrine	Xenobiotics	0.37	0.16	0.40	0.15	**0.02**
	Leucylalanine	Peptide	0.31	0.33	0.30	0.22	**0.02**
	Adenine	Nucleotide	0.29	0.22	0.36	0.30	**0.02**
	Adenosine 2'-monophosphate	Nucleotide	0.33	0.29	0.35	0.18	**0.02**
	3-(4-hydroxyphenyl)lactate	Amino acid	0.32	0.28	0.33	0.16	**0.02**
	O-acetylhomoserine	Amino acid	0.25	0.18	0.29	0.24	**0.03**
	Cotinine	Xenobiotics	0.39	0.28	0.37	0.07	**0.03**
	Arginylisoleucine	Peptide	0.25	0.19	0.40	0.27	**0.03**
	Tyramine	Amino acid	0.40	0.37	0.31	0.34	**0.04**
	3-phenylpropionate (hydrocinnamate)	Amino acid	0.27	0.22	0.26	0.05	**<0.05**
	Isoleucylisoleucine	Peptide	0.25	0.15	0.24	0.19	**<0.05**

Log of mean metabolites reported as raw concentrations. * unadjusted p-values used to compare peak of induction (Day 21) with baseline; only metabolites with $p < 0.05$ reported. † unadjusted p-values used to compare peak of resolution (Day 49) with peak of induction (Day 21); only metabolites with $p < 0.05$ reported. **Red values** indicated decreased metabolite levels from baseline to peak of induction (Day 21) and from peak of induction (Day 21) to peak of resolution (Day 49). **Blue values** indicated increased metabolite levels from baseline to peak of induction (Day 21) and from peak of induction (Day 21) to peak of resolution (Day 49).

APPENDIX 3.3. CHANGES IN METABOLITES THAT CO-VARY WITH CHANGES IN CLINICAL INDICES AT PEAK OF INDUCTION BY BGI CATEGORY (N = 50 TOTAL; N = 10 PER BGI CATEGORY)

BGI	Clinical Index	Metabolite	Super-pathway	Correlation Coefficient	*p*-value	*q*-value
H	PI	4-hydroxyphenylacetate	Amino acid	0.83	<0.01	0.44
		Glycylleucine	Peptide	0.79	0.01	0.44
		Chlorogenate	Xenobiotics	0.78	0.01	0.44
		Gallocatechin	Xenobiotics	0.75	0.01	0.44
		O-acetylserine	Amino acid	0.74	0.01	0.44
		3,4-dihydroxybenzoate	Xenobiotics	0.73	0.02	0.44
		Cortisone	Lipid	0.73	0.02	0.44
		2-oleoylglycerophosphoethanolamine	Lipid	0.72	0.02	0.44
		Histidine	Amino acid	0.71	0.02	0.44
		Isocaproate	Lipid	0.71	0.02	0.44
		5,6-dihydrothymine	Nucleotide	0.71	0.02	0.44
		glycerol 3-phosphate	Lipid	0.71	0.02	0.44
		Panose	Carbohydrate	-0.70	0.02	0.44
		2-hydroxyhippurate	Xenobiotics	-0.70	0.02	0.44
		Glucosamine	Carbohydrate	0.69	0.03	0.44
		Indolepropionate	Amino acid	0.69	0.03	0.44
		5,6-dihydrouracil	Nucleotide	0.69	0.03	0.44
		Adenine	Nucleotide	0.66	0.04	0.50
		2-aminobutyrate	Amino acid	0.66	0.04	0.50
		Creatine	Amino acid	0.65	0.04	0.50
		3-phenylpropionate	Amino acid	0.65	0.04	0.50
		Saccharin	Xenobiotics	0.65	0.04	0.50
	GI	p-cresol sulfate	Amino acid	0.84	<0.01	0.38
		Isocaproate	Lipid	0.83	<0.01	0.38
		Glycerate	Carbohydrate	0.81	<0.01	0.38
		7-methylxanthine	Xenobiotics	0.77	0.01	0.50
		N-acetylaspartate	Amino acid	0.77	0.01	0.50
		Leucylphenylalanine	Peptide	0.76	0.01	0.50
		Pinitol	Lipid	0.72	0.02	0.69
		Guanosine	Nucleotide	0.69	0.03	0.69
		Histidine	Amino acid	0.69	0.03	0.69
		Heptaethylene glycol	Xenobiotics	0.69	0.03	0.69
		Creatine	Amino acid	0.68	0.03	0.69
		3-phenylpropionate	Amino acid	0.67	0.04	0.71
		Caffeine	Xenobiotics	0.67	0.04	0.71
		Leucylglycine	Peptide	0.64	0.05	0.72
		Glucosamine	Carbohydrate	0.63	0.05	0.72

BOP	Butyrylcarnitine	Lipid	0.75	0.01	0.72
	Saccharin	Xenobiotics	0.73	0.02	0.72
	Gallocatechin	Xenobiotics	0.71	0.02	0.72
	linolenate	Lipid	0.70	0.02	0.72
	Glycyltyrosine	Peptide	0.70	0.03	0.72
	2-methylbutyroylcarnitine	Amino acid	0.70	0.03	0.72
	Glutamate	Amino acid	0.69	0.03	0.72
	Dihomo-linolenate	Lipid	-0.68	0.03	0.72
	Carnitine	Lipid	0.67	0.04	0.72
	Alpha-hydroxyisovalerate	Amino acid	0.66	0.04	0.72
	3-methyl-2-oxobutyrate	Amino acid	-0.65	0.04	0.72
	Glutamine	Amino acid	0.64	0.04	0.72
	Mannitol	Carbohydrate	0.64	0.05	0.72
PD	5-aminovalerate	Amino acid	0.86	<0.01	0.19
	Epicatechin	Xenobiotics	-0.84	<0.01	0.19
	1-kestose	Xenobiotics	-0.84	<0.01	0.19
	Glycerol	Lipid	-0.82	<0.01	0.19
	Arabinose	Carbohydrate	-0.80	0.01	0.19
	Gamma-aminobutyrate	Amino acid	-0.80	0.01	0.19
	3-(4-hydroxyphenyl)propionate	Amino acid	-0.79	0.01	0.19
	N6-acetyllysine	Amino acid	-0.79	0.01	0.19
	Isovalerate	Lipid	-0.78	0.01	0.19
	N-acetylputrescine	Amino acid	-0.78	0.01	0.19
	Serylisoleucine	Peptide	0.78	0.01	0.19
	Acetylsalicylate	Xenobiotics	-0.76	0.01	0.22
	Tryptophan	Amino acid	0.75	0.01	0.23
	Trans-urocanate	Amino acid	-0.72	0.02	0.36
	Maltose	Carbohydrate	0.68	0.03	0.53
	Hexaethylene glycol	Xenobiotics	-0.66	0.04	0.57
	Catechol sulfate	Xenobiotics	-0.66	0.04	0.57
	Hypoxanthine	Nucleotide	-0.64	0.04	0.63
	Chlorogenate	Xenobiotics	0.64	0.05	0.63
CAL	3-methylxanthine	Xenobiotics	-0.84	<0.01	0.46
	Carnitine	Lipid	-0.81	<0.01	0.46
	Sucralose	Carbohydrate	0.78	0.01	0.46
	Serylleucine	Peptide	0.77	0.01	0.46
	Cis-urocanate	Amino acid	-0.77	0.01	0.46
	Adenine	Nucleotide	-0.73	0.02	0.46
	Citrulline	Amino acid	-0.72	0.02	0.46
	Quinate	Xenobiotics	0.70	0.02	0.46
	Naringenin	Xenobiotics	-0.70	0.02	0.46
	Chiro-inositol	Lipid	0.70	0.02	0.46
	Mannitol	Carbohydrate	-0.70	0.03	0.46

		13-methylmyristic acid	Lipid	-0.69	0.03	0.46
		Lignocerate (24:0)	Lipid	0.69	0.03	0.46
		5,6-dihydrouracil	Nucleotide	-0.68	0.03	0.46
		Cyclo(phe-pro)	Peptide	-0.68	0.03	0.46
		Cinnamate	Xenobiotics	-0.68	0.03	0.46
		Glycyltyrosine	Peptide	-0.67	0.03	0.46
		Benzoate	Xenobiotics	-0.67	0.03	0.46
		Glycylleucine	Peptide	-0.66	0.04	0.46
		Glutarate	Amino acid	0.65	0.04	0.46
		3-(2-pyrrolidinyl)pyridine	Xenobiotics	-0.64	0.04	0.46
		Isoleucylisoleucine	Peptide	0.64	0.05	0.46
G	PI	3-phosphoglycerate	Carbohydrate	0.84	<0.01	0.45
		Sedoheptulose-7-phosphate	Carbohydrate	0.82	<0.01	0.45
		Alpha-ketoglutarate	Energy	0.77	0.01	0.66
		Beta-hydroxyisovalerate	Amino acid	0.76	0.01	0.66
		Arachidonate (20:4n6)	Lipid	0.73	0.02	0.73
		Pseudoephedrine	Xenobiotics	0.72	0.02	0.73
		2-methylbutyroylcarnitine	Amino acid	0.72	0.02	0.73
		Cyclo(phe-pro)	Peptide	0.68	0.03	0.99
		3-phenylpropionate (hydrocinnamate)	Amino acid	0.66	0.04	0.99
	GI	Arachidonate (20:4n6)	Lipid	0.87	<0.01	0.26
		2-methylbutyroylcarnitine	Amino acid	0.80	0.01	0.75
		Stachydrine	Xenobiotics	0.74	0.01	1.00
		Benzoylecgonine	Xenobiotics	0.72	0.02	1.00
		5,6-dihydrouracil	Nucleotide	0.71	0.02	1.00
		Fructose	Carbohydrate	0.69	0.03	1.00
		3-methyl-2-oxobutyrate	Amino acid	-0.67	0.03	1.00
		Lysylleucine	Peptide	0.64	0.04	1.00
		Lathosterol	Lipid	0.64	0.05	1.00
		Alpha-ketoglutarate	Energy	0.64	0.05	1.00
	BOP	Guanidine	Nucleotide	0.88	<0.01	0.18
		Threitol	Carbohydrate	0.85	<0.01	0.26
		Gallate	Xenobiotics	0.82	<0.01	0.26
		Salicylate	Xenobiotics	-0.80	0.01	0.26
		Gallocatechin	Xenobiotics	0.78	0.01	0.26
		Leucylalanine	Peptide	0.78	0.01	0.26
		Cadaverine	Amino acid	0.77	0.01	0.26
		Fucose	Carbohydrate	0.77	0.01	0.26
		Glutamine	Amino acid	0.77	0.01	0.26
		Benzoate	Xenobiotics	0.76	0.01	0.28
		Choline	Lipid	0.75	0.01	0.28
		Threonylphenylalanine	Peptide	0.74	0.01	0.30

	Glycylleucine	Peptide	0.74	0.02	0.30
	Sucrose	Carbohydrate	0.73	0.02	0.32
	p-cresol sulfate	Amino acid	0.71	0.02	0.36
	Cortisone	Lipid	-0.69	0.03	0.36
	Cis-urocanate	Amino acid	0.69	0.03	0.36
	Phenylalanylleucine	Peptide	0.69	0.03	0.36
	Tryptophan	Amino acid	0.69	0.03	0.36
	Linoleate (18:2n6)	Lipid	-0.69	0.03	0.36
	Arginylisoleucine	Peptide	0.68	0.03	0.36
	Leucylglycine	Peptide	-0.68	0.03	0.37
	Cinnamate	Xenobiotics	0.67	0.03	0.37
	Trans-4-hydroxyproline	Amino acid	0.66	0.04	0.38
	Deoxycarnitine	Lipid	0.66	0.04	0.38
	Phenylalanine	Amino acid	0.66	0.04	0.38
	Choline phosphate	Lipid	0.66	0.04	0.38
	N1-Methyl-2-pyridone-5-carboxamide	Cofactors and vitamins	0.64	0.05	0.41
	Isovalerylcarnitine	Amino acid	0.64	0.05	0.41
PD	3-(4-hydroxyphenyl)propionate	Amino acid	0.83	<0.01	0.41
	N-acetylputrescine	Amino acid	0.83	<0.01	0.41
	Citrulline	Amino acid	-0.79	0.01	0.44
	Aspartame	Xenobiotics	-0.76	0.01	0.44
	2-hydroxybutyrate (AHB)	Amino acid	0.75	0.01	0.44
	Glucosamine	Carbohydrate	0.75	0.01	0.44
	3-(4-hydroxyphenyl)lactate	Amino acid	-0.74	0.01	0.44
	Beta-alanine	Amino acid	0.74	0.01	0.44
	3-phenylpropionate (hydrocinnamate)	Amino acid	-0.73	0.02	0.46
	Lactate	Carbohydrate	-0.69	0.03	0.65
	Pyroglutamine	Amino acid	0.69	0.03	0.65
	N-acetylglycine	Amino acid	-0.65	0.04	0.74
	Beta-hydroxyisovalerate	Amino acid	-0.64	0.04	0.74
	1,6-anhydroglucose	Carbohydrate	-0.64	0.05	0.74
	Isoleucylisoleucine	Peptide	-0.64	0.05	0.74
	Ethanolamine	Lipid	0.64	0.05	0.74
CAL	Allantoin	Nucleotide	-0.80	0.01	0.46
	2-hydroxy-3-methylvalerate	Amino acid	0.78	0.01	0.46
	3-(2-pyrrolidinyl)pyridine	Xenobiotics	0.78	0.01	0.46
	4-methyl-2-oxopentanoate	Amino acid	0.78	0.01	0.46
	Diphenhydramine	Xenobiotics	0.77	0.01	0.47
	1,6-anhydroglucose	Carbohydrate	-0.73	0.02	0.71
	Pipecolate	Amino acid	-0.71	0.02	0.71
	Heptaethylene glycol	Xenobiotics	0.71	0.02	0.71
	Trans-urocanate	Amino acid	0.68	0.03	0.71

		Metabolite	Category			
		Aspartame	Xenobiotics	-0.67	0.03	0.71
		2-hydroxybutyrate	Amino acid	0.67	0.03	0.71
		Cortisone	Lipid	-0.66	0.04	0.71
		Glycerate	Carbohydrate	-0.66	0.04	0.71
		N-acetylputrescine	Amino acid	0.65	0.04	0.71
		4-hydroxy-3-methoxybenzyl alcohol	Xenobiotics	-0.64	0.05	0.71
P1	PI	3-phosphoglycerate	Carbohydrate	0.71	0.02	0.96
	GI	2-aminoadipate	Amino acid	-0.67	0.03	1.00
		Cysteine	Amino acid	-0.66	0.04	1.00
		3-aminoisobutyrate	Nucleotide	0.64	0.05	1.00
	BOP	3-aminoisobutyrate	Nucleotide	0.92	<0.01	0.03*
		1,3-diaminopropane	Amino acid	0.91	<0.01	0.03*
		6'-sialyllactose	Carbohydrate	-0.80	0.01	0.50
		2-aminophenol	Amino acid	0.78	0.01	0.51
		Arabinose	Carbohydrate	0.76	0.01	0.58
		Cysteine	Amino acid	-0.74	0.01	0.59
		Glucose	Carbohydrate	-0.69	0.03	0.98
	PD	Naringenin	Xenobiotics	0.87	<0.01	0.26
		Cyclo(phe-pro)	Peptide	0.77	0.01	0.76
		Triethanolamine	Xenobiotics	0.77	0.01	0.76
		Indolepropionate	Amino acid	0.74	0.02	0.82
		Phenol sulfate	Amino acid	0.70	0.02	0.82
		Phenylalanylisoleucine	Peptide	-0.65	0.04	0.82
		Phosphoethanolamine	Lipid	0.64	0.05	0.82
	CAL	3-methylxanthine	Xenobiotics	-0.70	0.02	0.90
		Glycerol	Lipid	-0.67	0.03	0.90
		Pantothenate	Cofactors and vitamins	-0.65	0.04	0.90
		Lidocaine	Xenobiotics	0.64	0.05	0.90
P2	PI	Catechol sulfate	Xenobiotics	0.76	0.01	0.43
		5-aminovalerate	Amino acid	-0.75	0.01	0.43
		3-(2-pyrrolidinyl)pyridine	Xenobiotics	0.74	0.02	0.43
		Alpha-hydroxyisocaproate	Amino acid	0.72	0.02	0.43
		Isoleucylserine	Peptide	-0.71	0.02	0.43
		1,2-propanediol	Lipid	0.70	0.02	0.43
		3-methyl-2-oxobutyrate	Amino acid	0.70	0.02	0.43
		1-palmitoylplasmenylethanolamine	Lipid	0.69	0.03	0.43
		5-oxoproline	Amino acid	0.69	0.03	0.43
		1,3-diaminopropane	Amino acid	0.69	0.03	0.43
		1,5-anhydroglucitol (1,5-AG)	Carbohydrate	0.69	0.03	0.43
		2-hydroxy-3-methylvalerate	Amino acid	0.69	0.03	0.43
		3-dehydrocarnitine	Lipid	0.69	0.03	0.43
		12-HETE	Lipid	0.69	0.03	0.43

	1,6-anhydroglucose	Carbohydrate	0.69	0.03	0.43
	2-hydroxyglutarate	Lipid	0.69	0.03	0.43
	Arginine	Amino acid	0.68	0.03	0.43
	4-acetamidophenol	Xenobiotics	0.68	0.03	0.43
	Citrate	Energy	0.67	0.03	0.43
	3-(4-hydroxyphenyl)lactate	Amino acid	-0.67	0.03	0.43
	Mannitol	Carbohydrate	0.66	0.04	0.44
	1-kestose	Xenobiotics	-0.66	0.04	0.44
	2-aminoadipate	Amino acid	0.66	0.04	0.44
	Glycyltyrosine	Peptide	-0.65	0.04	0.44
	3-aminoisobutyrate	Nucleotide	0.64	0.05	0.45
	2-aminophenol	Amino acid	0.64	0.05	0.45
GI	3-(4-hydroxyphenyl)lactate	Amino acid	-0.67	0.04	0.98
BOP	5,6-dihydrothymine	Nucleotide	-0.76	0.01	0.88
	Phenylalanine	Amino acid	0.75	0.01	0.88
	Cotinine	Xenobiotics	-0.74	0.02	0.88
	Isovalerate	Lipid	-0.73	0.02	0.88
	Tryptophan	Amino acid	-0.72	0.02	0.88
	Adenosine 2'-monophosphate	Nucleotide	-0.71	0.02	0.88
	Histamine	Amino acid	-0.70	0.02	0.88
	2-hydroxybutyrate	Amino acid	-0.68	0.03	0.92
	5-aminovalerate	Amino acid	-0.66	0.04	0.92
	N-carbamoylaspartate	Amino acid	-0.63	0.05	0.92
	7-methylxanthine	Xenobiotics	-0.63	0.05	0.92
PD	Pentaethylene glycol	Xenobiotics	-0.88	<0.01	0.21
	Carnitine	Lipid	-0.85	<0.01	0.21
	Alpha-hydroxyisocaproate	Amino acid	0.81	<0.01	0.35
	Glycyltyrosine	Peptide	-0.75	0.01	0.78
	3-(4-hydroxyphenyl)lactate	Amino acid	-0.70	0.02	0.78
	Heptaethylene glycol	Xenobiotics	-0.69	0.03	0.78
	Catechol sulfate	Xenobiotics	0.68	0.03	0.78
	Isocaproate	Lipid	-0.68	0.03	0.78
	Cyclo(leu-pro)	Peptide	-0.65	0.04	0.78
	1-kestose	Xenobiotics	-0.65	0.04	0.78
	3-methylxanthine	Xenobiotics	-0.64	0.05	0.78
CAL	Phenol sulfate	Amino acid	0.85	<0.01	0.30
	Glutathione, oxidized	Amino acid	-0.82	<0.01	0.30
	Beta-hydroxyisovalerate	Amino acid	0.81	<0.01	0.30
	Linoleate (18:2n6)	Lipid	-0.81	<0.01	0.30
	Isovalerate	Lipid	-0.78	0.01	0.36
	adenosine 2'-monophosphate	Nucleotide	-0.77	0.01	0.36
	2-aminobutyrate	Amino acid	-0.72	0.02	0.54
	Glucosamine	Carbohydrate	-0.72	0.02	0.54

		Adenosine 5'-monophosphate	Nucleotide	-0.71	0.02	0.54
		7-methylxanthine	Xenobiotics	-0.71	0.02	0.54
		Saccharin	Xenobiotics	-0.69	0.03	0.54
		Glucose-6-phosphate	Carbohydrate	-0.68	0.03	0.54
		Galactose	Carbohydrate	-0.68	0.03	0.54
		Phenylalanylisoleucine	Peptide	-0.68	0.03	0.54
		Allantoin	Nucleotide	-0.68	0.03	0.54
		3,4-dihydroxybenzoate	Xenobiotics	-0.66	0.04	0.59
		Ccytidine diphosphate	Nucleotide	0.64	0.05	0.59
		Phosphoenolpyruvate	Carbohydrate	0.64	0.05	0.59
		Lysine	Amino acid	-0.64	0.05	0.59
P3	PI	Fructose-6-phosphate	Carbohydrate	0.80	0.01	0.85
		Pyruvate	Carbohydrate	-0.74	0.02	0.85
		2,3-dihydroxyisovalerate	Cofactors and vitamins	0.72	0.02	0.85
		N-acetylglycine	Amino acid	0.71	0.02	0.85
		Glycyltyrosine	Peptide	0.65	0.04	0.85
		Adenosine 5'-monophosphate	Nucleotide	0.64	0.05	0.85
		Acetylcarnitine	Lipid	-0.64	0.05	0.85
	GI	Sorbitol	Carbohydrate	-0.76	0.01	0.99
		Scyllo-inositol	Lipid	0.66	0.04	0.99
	BOP	Isoleucylisoleucine	Peptide	-0.83	<0.01	0.68
		Hydrochlorothiazide	Xenobiotics	0.80	0.01	0.73
		Palmitoyl sphingomyelin	Lipid	0.73	0.02	0.77
		Isovalerylcarnitine	Amino acid	-0.72	0.02	0.77
		Linolenate	Lipid	-0.71	0.02	0.77
		Threonine	Amino acid	0.68	0.03	0.77
		Heptaethylene glycol	Xenobiotics	0.67	0.03	0.77
		Ethanolamine	Lipid	-0.66	0.04	0.77
		5,6-dihydrothymine	Nucleotide	0.66	0.04	0.77
		Lignocerate	Lipid	0.65	0.04	0.77
		3-(2-pyrrolidinyl)pyridine	Xenobiotics	-0.65	0.04	0.77
		Trans-4-hydroxyproline	Amino acid	-0.64	0.04	0.77
		Isoleucylserine	Peptide	0.64	0.05	0.77
		Linoleate	Lipid	-0.64	0.05	0.77
	PD	1-palmitoylplasmenylethanolamine	Lipid	-0.85	<0.01	0.15
		Lysine	Amino acid	-0.85	<0.01	0.15
		Carnitine	Lipid	-0.82	<0.01	0.15
		N-acetylaspartate	Amino acid	0.80	0.01	0.15
		Thymine	Nucleotide	-0.80	0.01	0.15
		Fructose	Carbohydrate	-0.79	0.01	0.15
		Betaine	Amino acid	-0.79	0.01	0.15
		Allantoin	Nucleotide	-0.78	0.01	0.15

13-methylmyristic acid	Lipid	-0.77	0.01	0.15
Glucose	Carbohydrate	-0.77	0.01	0.15
12-HETE	Lipid	-0.77	0.01	0.15
Glycerol	Lipid	-0.77	0.01	0.15
4-methyl-2-oxopentanoate	Amino acid	-0.77	0.01	0.15
Phenyllactate	Amino acid	-0.77	0.01	0.15
Arabitol	Carbohydrate	0.77	0.01	0.15
Pentaethylene glycol	Xenobiotics	-0.77	0.01	0.15
Adenine	Nucleotide	-0.76	0.01	0.16
Mannitol	Carbohydrate	-0.75	0.01	0.16
Leucylglycine	Peptide	-0.75	0.01	0.16
Leucylalanine	Peptide	0.75	0.01	0.16
Homoserine	Amino acid	-0.74	0.01	0.16
Diphenhydramine	Xenobiotics	-0.74	0.01	0.16
Arginine	Amino acid	-0.74	0.01	0.16
Phenylalanine	Amino acid	0.74	0.02	0.16
Isovalerate	Lipid	-0.74	0.02	0.16
Caffeine	Xenobiotics	0.73	0.02	0.17
Hypotaurine	Amino acid	-0.72	0.02	0.18
Cortisone	Lipid	-0.72	0.02	0.18
3-(4-hydroxyphenyl)propionate	Amino acid	-0.71	0.02	0.18
4-acetamidophenol	Xenobiotics	-0.71	0.02	0.18
Lactate	Carbohydrate	-0.70	0.02	0.20
Malate	Energy	-0.70	0.03	0.20
Erythronate	Carbohydrate	-0.70	0.03	0.20
Glycerate	Carbohydrate	-0.69	0.03	0.20
Salicylate	Xenobiotics	-0.69	0.03	0.21
O-acetylhomoserine	Amino acid	0.68	0.03	0.21
Ribulose	Carbohydrate	0.68	0.03	0.21
Beta-alanine	Amino acid	-0.68	0.03	0.21
7-methylxanthine	Xenobiotics	-0.67	0.03	0.21
Glutathione, oxidized	Amino acid	-0.67	0.04	0.22
Taurine	Amino acid	-0.66	0.04	0.22
Cadaverine	Amino acid	0.66	0.04	0.22
Trigonelline (N'-methylnicotinate)	Cofactors and vitamins	-0.66	0.04	0.22
Leucylphenylalanine	Peptide	-0.66	0.04	0.22
Citrulline	Amino acid	-0.66	0.04	0.22
3-dehydrocarnitine	Lipid	-0.65	0.04	0.22
Glucosamine	Carbohydrate	0.64	0.05	0.24
Phenylalanylleucine	Peptide	0.64	0.05	0.24
Chlorogenate	Xenobiotics	0.64	0.05	0.24
Ribitol	Carbohydrate	-0.64	0.05	0.24

CAL	N-acetylgalactosamine	Carbohydrate	-0.89	<0.01	0.15
	Dihomo-linolenate (20:3n3 or n6)	Lipid	-0.86	<0.01	0.16
	Guanine	Nucleotide	-0.84	<0.01	0.19
	Alpha-tocopherol acetate	Cofactors and vitamins	-0.72	0.02	0.67
	Isoleucylisoleucine	Peptide	0.71	0.02	0.67
	Cyclo(leu-pro)	Peptide	-0.71	0.02	0.67
	2-aminophenol	Amino acid	-0.70	0.02	0.67
	4-hydroxyphenylacetate	Amino acid	-0.69	0.03	0.67
	Sucralose	Carbohydrate	-0.69	0.03	0.67
	3-methyl-2-oxovalerate	Amino acid	-0.68	0.03	0.67
	4-hydroxy-3-methoxybenzyl alcohol	Xenobiotics	-0.68	0.03	0.67
	Pyridoxate	Cofactors and vitamins	-0.68	0.03	0.67
	3-phosphoglycerate	Carbohydrate	-0.64	0.05	0.87
	Threonate	Cofactors and vitamins	0.64	0.05	0.87

Correlation coefficients were evaluated using covariance matrices to describe a correlation between changes in metabolites and changes in clinical indices by BGI category at peak of induction (Day 21). Correlations with $p < 0.05$ are reported in this table. *FDR-adjusted p-values ($q<0.05$).

REFERENCES

Albandar, J. M. (2011). Underestimation of periodontitis in NHANES surveys. *Journal of Periodontology*, 82(3), 337-341.

Albandar, J. M., Brunelle, J. A., & Kingman, A. (1999). Destructive periodontal disease in adults 30 years of age and older in the united states, 1988-1994. *Journal of Periodontology*, 70(1), 13-29.

Arce, R. M., Diaz, P. I., Barros, S. P., Galloway, P., Bobetsis, Y., Threadgill, D., & Offenbacher, S. (2010). Characterization of the invasive and inflammatory traits of oral campylobacter rectus in a murine model of fetoplacental growth restriction and in trophoblast cultures. *Journal of Reproductive Immunology*, 84(2), 145-153.

Barnes, V. M. (2010). Assessment of the effects of dentifrice on periodontal disease biomarkers in gingival crevicular fluid. *Journal of Periodontology*, 81(9), 1273-1279.

Barnes, V. M., Ciancio, S. G., Shibly, O., Xu, T., Devizio, W., Trivedi, H. M., . . . Jonsson, T. J. (2011). Metabolomics reveals elevated macromolecular degradation in periodontal disease. *Journal of Dental Research*, 90(11), 1293-1297.

Barnes, V. M., Scannapieco, F., Cervi, S., Panagakos, F., Devizio, W., Trivedi, H. M., . . . Guo, L. (2013, March). Biochemical signatures associated with periodontal disease progression and diabetes. IADR/AADR/CADR 2013 Annual Meeting, Seattle, WA.

Barnes, V. M., Teles, R., Trivedi, H. M., Devizio, W., Xu, T., Mitchell, M. W., . . . Guo, L. (2009). Acceleration of purine degradation by periodontal diseases. *Journal of Dental Research, 88(9), 851-855.*

Bickel, M., & Cimasoni, G. (1985). The pH of human crevicular fluid measured by a new microanalytical technique. *Journal of Dental Research*, 20(1), 35-40.

Burrell, R. C., & Walters, J. D. (2008). Distribution of systemic clarithromycin to gingiva. *Journal of Periodontology*, 79(9), 1712-1718.

Byun, J. A., Lee, S. H., Jung, B. H., Choi, M. H., Moon, M. H., & Chung, B. C. (2008). Analysis of polyamines as carbamoyl derivatives in urine and serum by liquid chromatography-tandem mass spectrometry. *Biomedical Chromatography* : BMC, 22(1), 73-80.

Chae, Y. C., Angelin, A., Lisanti, S., Kossenkov, A. V., Speicher, K. D., Wang, H., . . . Altieri, D. C. (2013). Landscape of the mitochondrial Hsp90 metabolome in tumours. *Nature Communications*, 4, 2139.

Dunn, W. B., Goodacre, R., Neyses, L., & Mamas, M. (2011). Integration of metabolomics in heart disease and diabetes research: Current achievements and future outlook. *Bioanalysis*, 3(19), 2205-2222.

Dunn, W. B., Wilson, I. D., Nicholls, A. W., & Broadhurst, D. (2012). The importance of experimental design and QC samples in large-scale and MS-driven untargeted metabolomic studies of humans. *Bioanalysis*, 4(18), 2249-2264.

Eke, P. I., Dye, B. A., Wei, L., Thornton-Evans, G. O., Genco, R. J., & CDC Periodontal Disease Surveillance workgroup: James Beck (University of North Carolina, Chapel Hill, USA), Gordon Douglass (Past President, American Academy of Periodontology), Roy Page (University of Washin. (2012). Prevalence of periodontitis in adults in the united states: 2009 and 2010. *Journal of Dental Research*, 91(10), 914-920.

Evans, A. M., Mitchell, M. W., Dai, H., & DeHaven, C. D. (2012). Categorizing ion – features in liquid Chromatography/Mass spectrometry metobolomics data. *Metabolomics*, 2(3), 1-8.

Fiehn, O., Wohlgemuth, G., Scholz, M., Kind, T., Lee do, Y., Lu, Y., . . . Nikolau, B. (2008). Quality control for plant metabolomics: Reporting MSI-compliant studies. *The Plant Journal : For Cell and Molecular Biology*, 53(4), 691-704.

Galli, C., Passeri, G., & Macaluso, G. M. (2011). FoxOs, wnts and oxidative stress-induced bone loss: New players in the periodontitis arena? *Journal of Periodontal Research*, 46(4), 397-406.

Harding, J. J., Hassett, P. C., Rixon, K. C., Bron, A. J., & Harvey, D. J. (1999). Sugars including erythronic and threonic acids in human aqueous humour. *Current Eye Research*, 19(2), 131-136.

Hasegawa, S., Ichiyama, T., Sonaka, I., Ohsaki, A., Okada, S., Wakiguchi, H., . . . Furukawa, S. (2012). Cysteine, histidine and glycine exhibit anti-inflammatory effects in human coronary arterial endothelial cells. *Clinical and Experimental Immunology*, 167(2), 269-274.

Heasman, P. A., Collins, J. G., & Offenbacher, S. (1993). Changes in crevicular fluid levels of interleukin-1 beta, leukotriene B4, prostaglandin E2, thromboxane B2 and tumour necrosis factor alpha in experimental gingivitis in humans. *Journal of Periodontal Research*, 28(4), 241-247.

Heijl, L., Rifkin, B. R., & Zander, H. A. (1976). Conversion of chronic gingivitis to periodontitis in squirrel monkeys. Journal of Periodontology, 47(12), 710-716.

Holt, S. C., & Ebersole, J. L. (2005). Porphyromonas gingivalis, treponema denticola, and tannerella forsythia: The "red complex", a prototype polybacterial pathogenic consortium in periodontitis. *Periodontology 2000*, 38, 72-122.

Jahn, M., Baynes, J. W., & Spiteller, G. (1999). The reaction of hyaluronic acid and its monomers, glucuronic acid and N-acetylglucosamine, with reactive oxygen species. Carbohydrate Research,321(3-4), 228-234.

Kaufman, E., & Lamster, I. B. (2002). The diagnostic applications of saliva--a review. *Critical Reviews in Oral Biology and Medicine : An Official Publication of the American Association of Oral Biologists*, 13(2), 197-212.

Kinane, D. F., & Hart, T. C. (2003). Genes and gene polymorphisms associated with periodontal disease. *Critical Reviews in Oral Biology and Medicine : An Official Publication of the American Association of Oral Biologists*, 14(6), 430-449.

Lawton, K. A., Berger, A., Mitchell, M., Milgram, K. E., Evans, A. M., Guo, L., . . . Milburn, M. V. (2008). Analysis of the adult human plasma metabolome. *Pharmacogenomics*, 9(4), 383-397.

Lee, B. L., New, A. L., & Ong, C. N. (2003). Simultaneous determination of tocotrienols, tocopherols, retinol, and major carotenoids in human plasma. *Clinical Chemistry*, 49(12), 2056-2066.

Lee, S. H., Suh, J. W., Chung, B. C., & Kim, S. O. (1998). Polyamine profiles in the urine of patients with leukemia. *Cancer Letters*, 122(1-2), 1-8.

Löe, H., Anerud, A., Boysen, H., & Morrison, E. (1986). Natural history of periodontal disease in man. rapid, moderate and no loss of attachment in sri lankan laborers 14 to 46 years of age. *Journal of Clinical Periodontology*, 13(5), 431-445.

Löe, H., & Silness, J. (1963). Periodontal disease in pregnancy. I. prevalence and severity. *Acta Odontologica Scandinavica*, 21, 533-551.

Löe, H., Theilade, E., & Jensen, S. B. (1965). Experimental gingivitis in man. *The Journal of Periodontology*, 36, 177-187.

Main, P. A., Angley, M. T., O'Doherty, C. E., Thomas, P., & Fenech, M. (2012). The potential role of the antioxidant and detoxification properties of glutathione in autism spectrum disorders: A systematic review and meta-analysis. *Nutrition & Metabolism*, 9, 35-7075-9-35.

Michalowicz, B. S., Diehl, S. R., Gunsolley, J. C., Sparks, B. S., Brooks, C. N., Koertge, T. E., . . . Schenkein, H. A. (2000). Evidence of a substantial genetic basis for risk of adult periodontitis. *Journal of Periodontology*, 71(11), 1699-1707.

Morris, M., & Watkins, S. M. (2005). Focused metabolomic profiling in the drug development process: Advances from lipid profiling. *Current Opinion in Chemical Biology*, 9(4), 407-412.

Nurjhan, N., Bucci, A., Perriello, G., Stumvoll, M., Dailey, G., Bier, D., . . . Gerich, J. (1995). Glutamine: A major gluconeogenic precursor and vehicle for interorgan carbon transport in man. *Journal of Clinical Investigation*, 95, 272-277.

Offenbacher, S., Barros, S., Mendoza, L., Mauriello, S., Preisser, J., Moss, K., . . . Aspiras, M. (2010). Changes in gingival crevicular fluid inflammatory mediator levels during the induction and resolution of experimental gingivitis in humans. *Journal of Clinical Periodontology*, 37(4), 324-333.

Offenbacher, S., Barros, S. P., Paquette, D. W., Winston, J. L., Biesbrock, A. R., Thomason, R. G., . . . Ho, B. (2009). Gingival transcriptome patterns during induction and resolution of experimental gingivitis in humans. *Journal of Periodontology*, 80(12), 1963-1982.

Offenbacher, S., Barros, S. P., Singer, R. E., Moss, K., Williams, R. C., & Beck, J. D. (2007). Periodontal disease at the biofilm-gingival interface. *Journal of Periodontology*, 78(10), 1911-1925.

Offenbacher, S., Collins, J. G., & Arnold, R. R. (1993). New clinical diagnostic strategies based on pathogenesis of disease. *Journal of Periodontal Research*, 28(6 Pt 2), 523-535.

Offenbacher, S. (1996). Periodontal diseases: Pathogenesis. *Annals of Periodontology*, 1(1), 821-878.

Page, R. C., & Kornman, K. S. (1997). The pathogenesis of human periodontitis: An introduction. *Periodontology 2000*, 14, 9-11.

Paige, L. (2007). A preliminary metabolomic analysis of older adults with and without depression. *International Journal of Geriatric Psychiatry*, 22, 418-423.

Papapanou, P. N., Abron, A., Verbitsky, M., Picolos, D., Yang, J., Qin, J., . . . Pavlidis, P. (2004). Gene expression signatures in chronic and aggressive periodontitis: A pilot study. *European Journal of Oral Sciences*, 112(3), 216-223.

Ramfjord, S. P. (1967). The periodontal disease index (PDI). *Journal of Periodontology*, 38(6), Suppl:602-10.

Rasmussen, D. D., Ishizuka, B., Quigley, M. E., & Yen, S. S. (1983). Effects of tyrosine and tryptophan ingestion on plasma catecholamine and 3,4-dihydroxyphenylacetic acid concentrations. *The Journal of Clinical Endocrinology and Metabolism*, 57(4), 760-763.

Ren, C. J., Zhang, Y., Cui, W. Z., & Mu, Z. M. (2013). Progress in the role of oxidative stress in the pathogenesis of type 2 diabetes. *Acta Physiologica Sinica*, 65(6), 664-673.

Ryals, J., Lawton, K., Stevens, D., & Milburn, M. (2007). Metabolon, Inc. *Pharmacogenomics*, 8(7), 863-866.

Sha, W., da Costa, K. A., Fischer, L. M., Milburn, M. V., Lawton, K. A., Berger, A., . . . Zeisel, S. H. (2010). Metabolomic profiling can predict which humans will develop liver dysfunction when deprived of dietary choline. *FASEB Journal : Official Publication of the Federation of American Societies for Experimental Biology*, 24(8), 2962-2975.

Silness, J., & Löe, H. (1964). Periodontal disease in pregnancy. ii. correlation between oral hygiene and periodontal condtion. *Acta Odontologica Scandinavica*, 22, 121-135.

Socransky, S. S., Haffajee, A. D., Goodson, J. M., & Lindhe, J. (1984). New concepts of destructive periodontal disease. *Journal of Clinical Periodontology*, 11(1), 21-32.

Southerland, J. H., Moss, K., Taylor, G. W., Beck, J. D., Pankow, J., Gangula, P. R., & Offenbacher, S. (2012). Periodontitis and diabetes associations with measures of atherosclerosis and CHD. *Atherosclerosis*, 222(1), 196-201.

Stevens, C. R., Millar, T. M., Clinch, J. G., Kanczler, J. M., Bodamyali, T., & Blake, D. R. (2000). Antibacterial properties of xanthine oxidase in human milk. *Lancet*, 356(9232), 829-830.

Sukumar, S., & Drizhal, I. (2007). Hyaluronic acid and periodontitis. *Acta Medica (Hradec Kralove) / Universitas Carolina, Facultas Medica Hradec Kralove*, 50(4), 225-228.

Takahashi, N., Sato, T., & Yamada, T. (2000). Metabolic pathways for cytotoxic end product formation from glutamate- and aspartate-containing peptides by porphyromonas gingivalis. *Journal of Bacteriology*, 182(17), 4704-4710.

Trombelli, L., Tatakis, D. N., Scapoli, C., Bottega, S., Orlandini, E., & Tosi, M. (2004). Modulation of clinical expression of plaque-induced gingivitis. II. identification of "high-responder" and "low-responder" subjects. *Journal of Clinical Periodontology*, 31(4), 239-252.

van Gennip, A. H., van Bree-Blom, E. J., Abeling, N. G., van Erven, A. J., & Voute, P. A. (1987). Beta-aminoisobutyric acid as a marker of thymine catabolism in malignancy. *Clinica Chimica Acta; International Journal of Clinical Chemistry*, 165(2-3), 365-377.

van Kuilenburg, A. B., Meinsma, R., Beke, E., Assmann, B., Ribes, A., Lorente, I., . . . van Gennip, A. H. (2004). Beta-ureidopropionase deficiency: An inborn error of pyrimidine degradation associated with neurological abnormalities. *Human Molecular Genetics*, 13(22), 2793-2801.

Williams, R. C., & Offenbacher, S. (2000). Periodontal medicine: The emergence of a new branch of periodontology. *Periodontology 2000*, 23(1), 9-12.

Wu, R. Q., Zhao, X. F., Wang, Z. Y., Zhou, M., & Chen, Q. M. (2011). Novel molecular events in oral carcinogenesis via integrative approaches. *Journal of Dental Research*, 90(5), 561-572.